Title: The dorsal fan-shaped body is a neurochemically heterogeneous sleep-regulating center in *Drosophila*

Short Title: the dFB regulates sleep in *Drosophila*

Authors:

Joseph D. Jones[1#], Brandon L. Holder[1#], Andrew C. Montgomery[1], Chloe V. McAdams[1], Emily He[1], Anna E. Burns[1], Kiran R. Eiken[1], Alex Vogt[1], Adriana I. Velarde[1], Alexandra J. Elder[1], Jennifer A. McEllin[1] and Stephane Dissel[1*]

Affiliations:

[1]Division of Biological and Biomedical Systems, School of Science and Engineering, University of Missouri-Kansas City, Kansas City, Missouri, United States of America

co-first authors

[*]dissels@umkc.edu

Author contributions:

Conceptualization: SD

Methodology: SD, JDJ, BLH, ACM, JAM

Investigation: JDJ, BLH, ACM, CVM, EH, AEB, KRE, AV, AIV, AJE, JAM, SD

Visualization: JDJ, BLH, ACM, JAM, SD

Funding acquisition: SD

Project administration: SD

Supervision: SD

Writing – original draft: SD, JDJ, BLH, ACM, JAM

Writing – review & editing: SD, JDJ, BLH, ACM, JAM

Abstract: Sleep is a behavior that is conserved throughout the animal kingdom. Yet, despite extensive studies in humans and animal models, the exact function or functions of sleep remain(s) unknown. A complicating factor in trying to elucidate the function of sleep is the complexity and multiplicity of neuronal circuits that are involved in sleep regulation. It is conceivable that distinct sleep-regulating circuits are only involved in specific aspects of sleep and may underlie different sleep functions. Thus, it would be beneficial to assess the contribution of individual circuits in sleep's putative functions. The intricacy of the mammalian brain makes this task extremely difficult. However, the fruit fly *Drosophila melanogaster*, with its simpler brain organization, available connectomics, and unparalleled genetics offers the opportunity to interrogate individual sleep-regulating centers. In *Drosophila*, neurons projecting to the dorsal Fan-Shaped Body (dFB) have been proposed to be key regulators of sleep, particularly sleep homeostasis. We recently demonstrated that the most widely used genetic tool to manipulate dFB neurons, the 23E10-GAL4 driver, expresses in two sleep-regulating neurons (VNC-SP neurons) located in the Ventral Nerve Cord (VNC), the fly analog of the vertebrate spinal cord. Since most data supporting a role for the dFB in sleep regulation have been obtained using 23E10-GAL4, it

is unclear whether the sleep phenotypes reported in these studies are caused by dFB neurons or VNC-SP cells. A recent publication replicated our finding that 23E10-GAL4 contains sleep-promoting neurons in the VNC. However, it also proposed that the dFB is not involved in sleep regulation at all, but this suggestion was made using genetic tools that are not dFB-specific and a very mild sleep deprivation protocol. In this study, using a newly created dFB-specific genetic driver line, we demonstrate that the majority of 23E10-GAL4 dFB neurons can promote sleep when activated and that these neurons are involved in sleep homeostasis. We also show that dFB neurons require stronger stimulation than VNC-SP cells to promote sleep. In addition, we demonstrate that dFB-induced sleep can consolidate Short-Term Memory (STM) into Long-Term Memory (LTM), suggesting that the benefit of sleep on memory is not circuit-specific. Finally, we show that dFB neurons are neurochemically heterogeneous and can be divided in 3 populations. Most dFB neurons express both glutamate and acetylcholine, while a minority of cells express only one of these two neurotransmitters. Importantly, dFB neurons do not express GABA, as previously suggested. Using neurotransmitter-specific dFB tools, our data also points at cholinergic dFB neurons as particularly potent at regulating sleep and sleep homeostasis.

Introduction

Understanding the neural basis of behavior is a major aspect of neurobiology. However, unequivocally assigning a behavior to a specific neuron or group of neurons is not a trivial task. The extreme complexity, diversity, and connectivity of the mammalian nervous system renders this task even more daunting. To study the neural basis of a behavior, an investigator must be able to specifically manipulate a distinct group of cells and monitor the behavior of interest. Such approaches require precise genetic tools that allow for the manipulation of discrete neurons or

groups of neurons. While such tools exist in mammalian systems (1), they may not be available for all the diverse types of cells that underlie a specific behavior. It is therefore not surprising that animal models have been extensively used to untangle the neural basis of many different complex behaviors (2). One such model is the fruit fly *Drosophila melanogaster,* in which multiple binary systems have been developed to access and manipulate specific groups of neurons in the fly nervous system: GAL4/UAS (3), LexA/LexAop (4), and QF/QUAS (5). Of these 3 systems, the GAL4/UAS system has been by far the most extensively used. However, the expression patterns of GAL4 drivers are often not restricted enough to clearly link a behavior to specific neurons. In such cases, refinement of GAL4 expression pattern can be achieved by employing the intersectional Split-GAL4 technology (6).

Sleep is a behavior that has been observed in a multitude of species ranging from jellyfish to humans (7). A priori, sleep could appear to be a detrimental activity as it competes with other motivated behaviors, such as feeding, mating, or parenting, and renders organisms defenseless against potential predators. Despite these negative outcomes, sleep has been maintained throughout evolution, emphasizing its essential value (8). Sleep is regulated by two processes, the circadian clock which gates the occurrence of sleep and the sleep homeostat which controls the intensity and duration of sleep in response to prior wakefulness (9). Since the first characterization of sleep in *Drosophila* (10, 11), multiple studies have emphasized a high level of conservation of sleep mechanisms and regulation between flies and mammals (12). Like the mammalian system, sleep-regulating centers are found in many areas in the *Drosophila* brain (12, 13). Among them, neurons that project to the dorsal Fan-Shaped body (dFB) have attracted a lot of attention. Previous studies demonstrated that increasing the activity of neurons contained

in the C5-GAL4, 104y-GAL4, and C205-GAL4 drivers strongly promotes sleep (14, 15). While the expression patterns of these 3 independent drivers are broad, they show prominent overlap in the dFB (14). Based on these observations, the authors concluded that it is likely that the dFB plays a role in regulating sleep but could not rule out a role for neurons outside the dFB (14). In addition, further studies established that reducing the excitability of 104y-GAL4 neurons decreases sleep (16, 17). Highlighting the strong interaction between sleep and memory, activation of 104y-GAL4 neurons consolidates Short-Term Memory (STM) to Long-Term Memory (LTM) (14, 18) and restores STM in the classical memory mutants *rutabaga* and *dunce* (19). Further work supported a role for the dFB in sleep homeostasis by demonstrating that sleep deprivation increases the excitability of 104y-GAL4 dFB neurons (16). Taken together, these data pointed at 104y-GAL4 expressing neurons, most likely dFB cells, as important modulators of sleep. However, it was demonstrated that 104y-GAL4 also expresses in neurons projecting to the ventral Fan-Shaped body (vFB) and that these neurons modulate sleep and are involved in the sleep dependent consolidation of STM into LTM (18), making the conclusions about the role of 104y-GAL4 dFB neurons uncertain. More recent studies using 23E10-GAL4, a more restrictive driver to manipulate and monitor dFB neurons (20, 21), proposed that increasing sleep pressure switches dFB neurons from an electrically silent to an electrically active state, and that this process is regulated by dopaminergic signaling to the dFB (20) and the accumulation of mitochondrial reactive oxygen species in dFB neurons (22). Because of their physiological properties, dFB neurons have been proposed to be the fly functional analog to the ventrolateral preoptic nucleus (VLPO), a key center regulating sleep homeostasis in the mammalian brain (16, 23).

Chronic and acute activation of 23E10-GAL4 neurons increases sleep (18, 24-28). Since it has a relatively restricted expression pattern and a strong capacity to modulate sleep, 23E10-GAL4 (as it relates to sleep) is seen as a dFB-specific driver by most in the scientific community. However, our recent work, aimed at identifying individual sleep-regulating 23E10-GAL4 expressing neurons, demonstrated that this driver is not as dFB-specific as previously believed. In particular, we demonstrated that 23E10-GAL4 expresses in two cholinergic sleep-promoting cells (VNC-SP neurons) located in the Ventral Nerve Cord (VNC) (27). Additional work from another laboratory confirmed that there are VNC-localized sleep-promoting neurons in the 23E10-GAL4 driver (28). Together, these findings have raised some serious questions about the role, if any, of the dFB in sleep regulation, especially if these data were obtained using 23E10-GAL4. In fact, two recent studies suggest that the dFB has no sleep-regulating capacity (28, 29). However, for one of this study, the conclusions made by the authors are based on data obtained with non dFB-specific tools and a very mild sleep deprivation protocol (28). The second study employed a very brief and mild optogenetic activation of all 23E10-GAL4 neurons (29). In the current study, we sought to unequivocally assess the role of the dFB in sleep regulation by conducting a targeted, intersectional Split-GAL4 screen (6) focused on 23E10-GAL4 dFB neurons. We report here that sleep-promoting VNC-SP neurons are present in most Split-GAL4 lines we created, making it difficult to assess the role of the dFB using these lines. However, we identified a dFB-specific Split-GAL4 line that can be used to manipulate most 23E10-GAL4 dFB neurons. Using this novel driver, we demonstrate that 23E10-GAL4 dFB cells regulate sleep, especially sleep homeostasis, and that this dFB-induced sleep promotes the consolidation of STM to LTM. In addition, our work reveals that dFB neurons are neurochemically heterogeneous and that cholinergic dFB neurons play an important role in sleep regulation.

Results

A dFB-based Split-GAL4 screen identifies multiple sleep-promoting lines

To assess the role of 23E10-GAL4 dFB neurons in sleep regulation, we designed a Split-GAL4 screen (6) focused on the dFB. The Split-GAL4 technology separates the functional GAL4 transcription factor into two non-functional fragments, a GAL4 DNA-binding domain (DBD) and an activation domain (AD). Expression of the AD and DBD fragments is controlled by different enhancers and the functional GAL4 transcription factor is reconstituted only in the cells in which both fragments are expressed (6). We obtained 20 different AD lines based on their associated GAL4 line's expression in the dFB, as observed using the Janelia Flylight website (21, 30). Since the goal of our screen was to identify the contribution of 23E10-GAL4 dFB neurons in sleep regulation, we designed a targeted approach by combining these individual AD lines to a 23E10-DBD line (30, 31), thus creating 20 new Split-GAL4 lines named FBS for Fan-Shaped Body Splits (See S1 Table for a description of these lines). These newly created lines were screened behaviorally for their ability to modulate sleep and anatomically to identify their expression patterns. Each individual Split-GAL4 FBS line was crossed to: 1) a line expressing both the thermogenetic TrpA1 cation channel (32) and an mCD8GFP construct and 2) the optogenetic CsChrimson actuator (33).

For the thermogenetic screen, flies were maintained at 22°C for 2 days before raising the temperature to 31°C at the beginning of day 3 for a duration of 24h. Temperature was then lowered to 22°C on day 4 for recovery (Fig 1A). For each individual fly, we calculated the percentage of total sleep change between activation day (day3) and baseline day (day2) (Fig 1A).

As a control for this screen, we used an enhancerless AD construct (created in the vector used to make all the AD lines) combined with 23E10-DBD, since it is the common element in all the Split-GAL4 lines analyzed in this screen. As seen in Fig 1B, acute thermogenetic activation of the neurons contained in 4 of the 20 FBS lines led to significant increases in sleep in female flies (FBS42, FBS45, FBS53, FBS68), when compared with controls. Individual sleep traces for these 4 lines are shown in Fig 1D-1H. Sleep profiles of the other 16 FBS lines are shown in S1 Fig. Importantly, analysis of activity counts during awake time reveals that increases in sleep are not caused by a reduction in locomotor activity (S2A Fig), ruling out motor deficits or paralysis. On the contrary, 2 of the sleep-inducing lines even showed an increase in waking activity upon neuronal activation. While increases in total sleep are indicative of increased sleep quantity, this measurement does not provide information about sleep quality or sleep depth. Previous work proposed that increased sleep bout duration is an indication of increased sleep depth (34). To assess whether sleep quality is modulated when activating FBS lines, we analyzed sleep consolidation during the day and night in these flies. As seen in S2B Fig, daytime sleep bout duration is significantly increased upon thermogenetic activation in 7 out of 20 FBS lines (FBS28, FBS42, FBS45, FBS53, FBS68, FBS72, and FBS84). Interestingly, 3 of those 7 lines did not show an increase in total sleep (FBS28, FBS72, and FBS84). During the nighttime, the effect of high temperature on sleep is obvious as most lines, including the control, display a significant decrease in sleep bout duration when raising the temperature to 31°C (S2C Fig). These data agree with previous studies documenting that changes in temperature modulate sleep architecture and that high temperature disturbs sleep at night (35-38) . Only 4 of the 20 FBS lines (FBS42, FBS45, FBS53, and FBS68) maintain similar nighttime sleep bout durations before and

during thermogenetic activation. Importantly, in 3 of these 4 lines, nighttime sleep bout duration is significantly increased at 31°C when compared to control flies (S2C Fig).

Since sleep in *Drosophila* is sexually dimorphic (39-41), we systematically assessed male flies in our experiments. As seen in S3A Fig, thermogenetic activation increases total sleep in males in 7 out of the 20 FBS lines, including the 4 lines that increase total sleep in females (FBS42, FBS45, FBS53, FBS68, FBS72, FBS81, and FBS84). These effects on total sleep are not caused by motor deficits or paralysis as waking activity is not reduced in long sleeping male flies (S3B Fig). Daytime sleep bout duration is significantly increased in 6 out of these 7 lines (S3C Fig). When examining nighttime sleep, thermogenetic activation of FBS45 and FBS68 significantly increases bout duration while FBS42, FBS53, FBS81, and FBS84 show no difference between 22°C and 31°C (S3D Fig). Altogether, our thermogenetic approach identified 8 FBS lines that increase total sleep and/or sleep bout duration when activated (S2 Table).

Because of the strong effect that temperature has on sleep, we sought to confirm our thermogenetic findings using an alternative method to manipulate FBS lines. The logic behind our thinking is that it may be difficult to fully describe and characterize the sleep behaviors of our FBS lines when temperature itself has such a profound effect on sleep. Furthermore, a recent study demonstrated that some of the effects of high temperature on sleep are mediated by GABAergic transmission on dFB neurons (38). We thus undertook an optogenetic screen using CsChrimson (33). Our optogenetic experimental setup is described in Fig 1A. Notably, for neurons to be activated when expressing CsChrimson, flies need to be fed all trans-retinal and the neurons must be stimulated with a 627nm LED light source (33). Thus, optogenetic approaches provide a much better control on the timing and parameters of activation. Our

optogenetic activation screen gave results that are mostly identical to the thermogenetic approach. That is, all 4 sleep-promoting lines identified using TrpA1 also increase total sleep when activated with CsChrimson in retinal-fed female flies (FBS42, FBS45, FBS53, and FBS68) (Fig 1C). Interestingly, activation of neurons contained in FBS70 and FBS72 is sleep-promoting in retinal-fed female flies while it was not using TrpA1 (Fig 1B and 1C). Sleep profiles of all FBS lines subjected to optogenetic activation are shown in S4 Fig. Looking at males, optogenetic activation increases total sleep in all 7 sleep-promoting lines identified using TrpA1 (FBS42, FBS45, FBS53, FBS68, FBS72, FBS81, and FBS84), as well as an 8th line (FBS33) (S5A Fig). Importantly, these optogenetic sleep-promoting effects are not the result of locomotor deficits (S5B Fig for males and S6A Fig for females).

Examination of sleep bout duration in retinal-fed flies indicates that most sleep-promoting FBS lines increase sleep consolidation during the day (S5C Fig for males and S6B Fig for females) and during the night (S5D Fig for males and S6C Fig for females). Interestingly, some FBS lines that did not increase total sleep upon optogenetic activation increased daytime sleep bout duration in females (FBS57, FBS60, FBS81, and FBS84) (S6B Fig) and in males (FBS35, FBS64, and FBS87) (S5C Fig). In addition, optogenetic activation of neurons contained within FBS58 increases nighttime sleep bout duration in females (S6C Fig). These data suggest that these lines may also express in sleep-regulating neurons. Importantly, analysis of sleep parameters in vehicle-fed flies demonstrate that the sleep phenotypes we observed are specific to retinal-fed and LED stimulated flies (S7 Fig for females and S8 Fig for males).

A summary of sleep-modulating effects for all FBS lines in both activation protocols is provided in S2 Table. Taken together, our thermogenetic and optogenetic screens revealed that activating

neurons contained within 16 FBS lines increases at least one sleep parameter. Among these 16 lines, 7 are consistently increasing total sleep and sleep consolidation in females and males using both activation protocols (FBS42, FBS45, FBS53, FBS68, FBS72, FBS81, and FBS84) (S2 Table).

VNC-SP neurons are present in most FBS lines

Having identified 16 different Split-GAL4 lines that significantly increase at least one sleep parameter when thermogenetically or optogenetically activated, we sought to identify the neurons that are contained within these lines. As seen in Fig 1D-1H and S1 Fig, 19 out of 20 lines express in dFB neurons, with only FBS25 showing no expression at all in the brain and VNC. Since FBS25 expresses in no neurons at all, it is not surprising that no sleep changes were seen using both activation protocols, as FBS25 should behave like a control. The number of dFB neurons contained within different FBS lines ranges from 4 to 27 per brain on average (S1 Table). Most lines show very little additional expression in the brain and there is no consistency in these non-dFB labeled cells between different lines. However, 18 out of the 19 lines that express in dFB neurons also express in cells in the metathoracic ganglion of the VNC. This is not surprising as our previous study showed that the 23E10-GAL4 driver, on which this Split-GAL4 screen is based, expresses in 4 neurons located in the metathoracic ganglion of the VNC, consisting of 2 TPN1 neurons (42) and the two VNC-SP cells (27). Most FBS lines (17) express in neurons that have anatomical features similar to VNC-SP neurons in the VNC and in the brain, including very typical processes that we previously named “bowtie” (27). These “bowtie” processes are located extremely close to the axonal projections of dFB neurons, making their visualization sometimes difficult depending on the strength of dFB projections’ staining.

Importantly, all 16 FBS lines that increase at least one sleep parameter when activated express in these VNC-SP-like cells, in addition to dFB neurons. Furthermore, most FBS lines (14) also express in cells that appear to be TPN1 neurons (42).

Our previous study demonstrated that VNC-SP neurons are cholinergic and that the expression of the Split-GAL4 repressor KZip^{+} (43) under the control of a ChAT-LexA driver effectively blocks the accumulation of reconstituted GAL4 in VNC-SP neurons (27). Since we observed neurons reminiscent of VNC-SP in all 4 FBS lines that increase sleep when thermogenetically activated in females, we wondered whether VNC-SP neurons are the cells responsible for the sleep increase in these lines. To address this possibility, we expressed TrpA1 and GFP in FBS42, FBS45, FBS53, and FBS68 neurons while simultaneously driving the expression of the KZip^{+} repressor in ChAT-LexA cells. As seen in S9A-S9D Fig, expressing the KZip^{+} repressor in cholinergic cells abolishes GFP expression in the metathoracic ganglion in all *FBS>UAS-GFP; ChAT-LexA>LexAop2-KZip*$^{+}$ flies. These data demonstrate that VNC-SP neurons are present in the expression pattern of all 4 FBS lines tested. When assessing sleep, expressing the KZip^{+} repressor in ChAT-LexA cells prevents the increase in sleep seen in all *FBS>UAS-TrpA1* flies tested (S9E Fig). These data suggest that the neurons responsible for the sleep increase observed when thermogenetically activating FBS42, FBS45, FBS53, and FBS68 cells are the cholinergic VNC-SP neurons. However, since we previously demonstrated that some 23E10-GAL4 dFB neurons are cholinergic (27), it is possible that cholinergic 23E10-GAL4 dFB neurons may also participate in these sleep phenotypes. Based on these data, and our previous work showing that 23E10-GAL4 expresses in VNC-SP cells (27), we believe that all 16 FBS sleep-promoting lines

express in VNC-SP neurons, making it impossible for us to assess whether 23E10-GAL4 dFB neurons modulate sleep using these lines.

However, if VNC-SP neurons are present in most FBS lines, why do not we see any sleep changes with one of them (FBS1)? In addition, why are some VNC-SP-expressing FBS lines more potent than others at promoting sleep? We hypothesized that these differences may be explained by differences in strength of expression of the reconstituted GAL4 in VNC-SP neurons in FBS lines. To address this, we used a GFP-DD construct which is normally degraded by the proteasome (44). Degradation is blocked when feeding the flies trimethoprim (TMP) (44) and therefore strength of expression can be assessed. We used 23E10-GAL4 and the VNC-SP Split-GAL4 line previously described (27) as controls to compare expression levels in the VNC-SP neurons of different FBS lines. Flies were maintained on standard food until they reached 5-6 days of age. Next, half of the flies were fed either vehicle control (DMSO) or TMP, to protect GFP-DD from degradation, for 24h (S10A Fig). Flies were then dissected and GFP levels were measured in the metathoracic ganglion of the VNC. As seen in S10B and S10C Fig, feeding TMP leads to strong increases in GFP signal in VNC-SP neurons when GFP-DD is expressed using 23E10-GAL4, VNC-SP Split, and FBS45. When GFP-DD is expressed in FBS33 cells, we observed a moderate increase in GFP signal intensity. With two lines, FBS1 and FBS58, we saw no statistical differences between DMSO-fed and TMP-fed flies. The strength of expression in VNC-SP neurons correlates well with the magnitude of sleep increases seen when activating the different lines (S2 Table). FBS45 is strongly sleep-promoting when thermogenetically and optogenetically activated, while FBS33 only increases total sleep and daytime sleep bout duration in males using optogenetic activation. Finally, FBS58 has a very modest impact on

sleep while FBS1 has none. Thus, we conclude that within our FBS lines, the strength of expression in VNC-SP neurons dictates how potently a given line can modulate sleep.

When combining behavioral and anatomical data, we conclude that the numbers of dFB neurons contained within a specific FBS line cannot be predictive of whether the line can strongly promote sleep upon neuronal activation. For example, FBS68 strongly increases all sleep parameters in both sexes and activation protocols while only expressing in 3-6 dFB neurons (Fig 1H, S1 and S2 Tables). Conversely, FBS60 contains 22-27 dFB neurons and only increases daytime sleep bout duration in females using optogenetic activation (S1J Fig, S1 and S2 Tables). The anatomical feature that is predictive of whether a FBS line can modulate sleep or not is the presence/absence of VNC-SP neurons within the pattern of expression. In addition, how strongly a line expresses in VNC-SP neurons dictates how strongly sleep-promoting that line is (S10B and S10C Fig).

In conclusion, our activation screens and anatomical analysis identified 16 sleep-promoting FBS lines expressing in diverse numbers of dFB neurons. However, all 16 lines contain the previously identified sleep-promoting VNC-SP neurons. Thus, these lines are not well suited to unequivocally assess the role of 23E10-GAL4 dFB neurons in sleep.

Identification of a dFB-specific Split-GAL4 line

In our screen, we only identified two FBS lines that express in dFB neurons but not in VNC-SP cells (FBS6 and FBS41). No sleep parameters are increased when activating neurons contained within either line. However, both lines only express in a reduced number of dFB neurons (S1 Fig

and S1 Table). Thus, these two lines are not fully recapitulating the dFB expression pattern of the 23E10-GAL4 driver. Fortunately, we identified an additional FBS line (84C10-AD; 23E10-DBD which we named dFB-Split) that expresses in 18-27 dFB neurons per brain and no other cells in the brain or VNC (Fig 2A, S1 and S2 Movies, S1 Table). Since we previously reported that 23E10-GAL4 reliably labels 23-30 dFB neurons in our confocal microscopy experiments (27), we conclude that dFB-Split expresses in 78-90% of 23E10-GAL4 dFB neurons. Additionally, dFB-Split does not express in the wings, legs, gut, or ovaries (S11 Fig). Though not being a complete replication of all 23E10-GAL4 dFB neurons, we hypothesized that the dFB-Split line is a good tool to assess a role for 23E10-GAL4 dFB neurons in sleep regulation. For clarity, we will refer to the dFB cells contained in the dFB-Split expression pattern as $dFB^{23E10\cap 84C10}$ neurons.

Activation of $dFB^{23E10\cap 84C10}$ neurons promotes sleep

Having identified a genetic driver that is dFB-specific and includes the majority of the 23E10-GAL4 dFB neurons, we sought to investigate the contribution of these cells to sleep. First, we employed a 1Hz optogenetic activation protocol and found no effects on sleep in female flies (Fig 2B and 2C). Next, we used our standard optogenetic protocol and again obtained no sleep increases when activating $dFB^{23E10\cap 84C10}$ neurons in females (Fig 2D and 2E)-. Note that this activation protocol is sufficient to increase sleep using multiple other drivers (Fig 1C) and the VNC-SP Split-GAL4 (27), indicating that it is effective at activating neurons. Why then does this protocol not cause an effect in $dFB^{23E10\cap 84C10}$ neurons? Previous studies have demonstrated that the dFB is under strong dopaminergic inhibition (15, 17, 20, 45) and that dopamine is a key factor regulating whether dFB neurons are active or silent (20). In addition, it was shown that

sleep deprivation increases the activity of dFB neurons, switching them to the active state (16). We hypothesize that in our experiments, sleep pressure is low, as flies are allowed to sleep normally before activation. Thus, the inhibitory activity of dopaminergic inputs to the dFB should be relatively strong and it is possible that our standard activation protocol may not be sufficient to overcome this inhibition. To test this possibility, we decided to increase the intensity of the optogenetic activation protocol. As seen in Fig 2F and 2G, a 10Hz activation of dFB$^{23E10\cap 84C10}$ neurons increases total sleep in females. In addition, it significantly increases daytime sleep bout duration (S12B Fig). These effects are not due to a locomotor deficit as waking activity is unaffected by 10Hz optogenetic activation in females (S12A Fig). Importantly, this increase in daytime sleep consolidation is not seen in vehicle-fed flies (S12E). We found similar sleep promoting effects when looking at *dFB-Split>CsChrimson* females and males subjected to a 20Hz optogenetic activation (Fig 2H and 2I for females and S13G Fig for males). In addition, a 20Hz optogenetic activation increases daytime and nighttime sleep bout duration in female and male flies (S13B and S13C Fig for females and S13I and S13J Fig for males). Again, these effects are not due to a locomotor deficit as waking activity is unaffected by a 20Hz activation (S13A Fig for females and S13H Fig for males).

We next used a 50Hz activation protocol. As seen in Fig 2J and 2K, total sleep is increased in *dFB-Split>CsChrimson* females when activated with a 50Hz protocol. Furthermore, daytime and nighttime sleep bout durations are increased in females using this activation protocol (S14B and S14C Fig). These effects are not the result of abnormal locomotor activity (S14A Fig) and are not seen in vehicle-fed flies (S14E and S14F Fig). Similar behavioral data was obtained when activating dFB$^{23E10\cap 84C10}$ neurons with a 50Hz optogenetic protocol in male flies (S14G-S14M

Fig). Since our data suggested a direct relationship between the intensity of the optogenetic activation protocol and the capacity of dFB$^{23E10\cap 84C10}$ neurons to increase sleep, we decided to turn the 627nm LEDs on constantly. As seen in Fig 2L, constant LED activation of dFB$^{23E10\cap 84C10}$ neurons significantly increases sleep in females, indicating that once the activation protocol is sufficient (above 10Hz), dFB$^{23E10\cap 84C10}$ neurons can reliably promote sleep.

Recent studies have proposed that activation of all 23E10-GAL4-expressing neurons (including dFB$^{23E10\cap 84C10}$ cells) promotes micromovements, such as grooming, rather than sleep (29, 46). It is important to note that these conclusions were made using either a thermogenetic approach that may not be sufficient (29° instead of the more commonly used 31° for TrpA1 activation) or a very brief (5 minutes) 1Hz optogenetic activation protocol. As mentioned above, we showed that a 24h long 1Hz optogenetic activation of dFB$^{23E10\cap 84C10}$ neurons was insufficient to increase sleep (Fig 2B and 2C). To further validate that sufficient optogenetic activation of dFB$^{23E10\cap 84C10}$ neurons increases sleep, and not any other behavior (feeding, grooming, or in-place micromovements) that could be falsely registered as sleep by the single beam DAM2 system, we employed the more sensitive multibeam activity monitors (DAM5H, Trikinetics). These monitors contain 15 independent infrared beams, separated by 3 mm across the tube length, resulting in flies being continuously monitored by at least one beam during the experiment. First, we sought to validate the sensitivity of the multibeam system to detect different behaviors. We loaded 19 wild-type *Cs* flies in 65mm long glass tubes and monitored behavior for 10 minutes using the multibeam system and video recording concurrently (S15A Fig). Video analysis revealed that flies always perform one of 7 different behaviors: rest (total immobility), walking (movement), feeding (micromovement), grooming (micromovement), posture change (a small

dip of the abdomen, micromovement), proboscis extension (micromovement), and single leg movement (micromovement) (S15B Fig, S3 and S4 Movies). Our analysis of the multibeam data obtained from the 19 flies revealed that when considering all 7 behaviors, the multibeam sensitivity is 88.9% (S15C Fig). When looking at individual behaviors, sensitivity is above 90% for rest, walking, feeding, and grooming (S15C Fig). However, the multibeam performs poorly for detection of posture change, proboscis extension, and single leg movement (S15C Fig). Notably, these 3 behaviors are extremely subtle with only a very minor movement of one body part, and do not resemble the jerky multiple legs movements that have been described for 1Hz activation of all 23E10-GAL4 neurons (29). Additionally, the accuracy of the multibeam system is above 90% for walking and micromovements and 78% for rest (S15C Fig).

Importantly, for walking, the 8.9% of walking events not picked by the multibeam system are scored as micromovements, so they are not falsely registered as rest. Taking this into account, it brings the sensitivity of the multibeam system for walking/micromovements to 91.5%. Missed feeding, grooming, posture change, proboscis extension, and single leg movement events are labelled as rest by the multibeam system.

Interestingly, we observed that posture change, proboscis extension, and single leg movement events are always surrounded by periods of rest (S15D Fig top panels and S15E Fig, bottom panels, S3 and S4 Movies). Previous studies have suggested that such events are associated with sleep (29, 47), suggesting that a failure of the multibeam system to detect them may not lead to a dramatic overestimation of sleep, especially considering the low frequency of such behaviors (S15B Fig). If we consider that posture change, proboscis extension, and single leg movement are part of sleep, the accuracy of the multibeam system for correctly picking up rest jump to 95.9% (S15C Fig).

Finally, for us to falsely label a period of micromovements that have not been associated with sleep (feeding or grooming) as sleep, we would need the multibeam to fail to detect any of these micromovements for 5 consecutive minutes, which is something we have not seen in the 190 minutes of data we analyzed. In addition, we only detected one occurrence where a failure to detect a feeding event would have led to the mislabeling of a 5min period as sleep for one of the flies. Thus, we conclude that the multibeam system is sensitive and accurate enough to detect micromovements that involve several body parts such as feeding and grooming, and that it is a valid tool to quantify sleep.

As seen in Fig 2M and 2N, 20Hz and 50Hz optogenetic activations significantly increase sleep in *dFB-Split>CsChrimson* females as assessed using the DAM5H multibeam system, ruling out the possibility that we misregistered micromovements as sleep.

However, to further support our findings, we performed video analysis. First, we coupled video and multibeam analysis of control and *dFB-Split>CsChrimson* females during 10 minutes of baseline recording and the subsequent 10 minutes of optogenetic activation at 20Hz (Fig 2O). We found that upon optogenetic activation of $dFB^{23E10\cap 84C10}$ neurons, walking is significantly reduced, and rest (total immobility with no micromovements) is increased (Fig 2P, S5-S18 Movies). Importantly, we observed no change in micromovements upon optogenetic activation (Fig 2P, S5-S18 Movies). Both multibeam and video analysis produced similar results, reinforcing the validity of the multibeam system to properly register sleep, movements, and micromovements (Fig 2P). Second, we performed video analysis of multiple behaviors before and during constant optogenetic activation of $dFB^{23E10\cap 84C10}$ neurons and we found that times spent feeding, grooming, and walking are significantly reduced in *dFB-Split>CsChrimson* flies during activation, while time spent sleeping is significantly increased (Fig 2Q). Thus, based on

our behavioral and video analysis, we conclude that activation of dFB$^{23E10\cap 84C10}$ neurons increases sleep, rather than micromovements.

Finally, we investigated whether activation of dFB$^{23E10\cap 84C10}$ neurons modulate arousal threshold by applying mechanical stimulations of increasing strength to *dFB-Split>CsChrimson* flies. As seen in Fig 2R, when dFB$^{23E10\cap 84C10}$ neurons are activated (retinal-fed, LED ON), a significantly lower percentage of flies are awakened by the 20% and 40% stimulus strength, compared with non-activated flies (retinal-fed, LED OFF). Importantly, at the higher stimuli strength (60%, 80%, and 100%), there are no differences between activated and non-activated *dFB-Split>CsChrimson* flies, indicating that these flies can respond to a stimulus of sufficient strength (i.e., these flies are not paralyzed). These data suggest that activation of dFB$^{23E10\cap 84C10}$ neurons increases arousal threshold, an indicator of sleep depth.

Thus, we conclude that sufficient activation of dFB$^{23E10\cap 84C10}$ neurons can increase sleep, sleep consolidation, and sleep depth.

The sleep induced by dFB$^{23E10\cap 84C10}$ neuronal activation consolidates STM to LTM

To further support that activation of dFB$^{23E10\cap 84C10}$ neurons increases sleep and not micromovements, we sought to assess whether the state induced by activation of dFB$^{23E10\cap 84C10}$ neurons can support one of sleep's proposed functions. The relationship between sleep and memory is well documented (13, 48, 49). In particular, sleep plays a role in the consolidation of STM into LTM (50). Employing genetic and pharmacological activation, previous studies have demonstrated that inducing sleep after a courtship memory training protocol sufficient to create STM, but not LTM, could convert that STM to LTM in *Drosophila* (14, 18, 19). Sleep depriving flies while activating sleep-promoting neurons abrogated the formation of LTM, demonstrating

that sleep was needed for this effect (14). More recent studies have shown that post-learning neuronal reactivation of dopaminergic neurons that are involved in memory acquisition is needed for LTM consolidation (18). Importantly, this reactivation necessitates sleep and the activity of vFB neurons during a narrow time window after learning (18, 51). Based on their data, the authors proposed that vFB and dFB neurons promote sleep in response to different types of experiences and that these neurons underlie different functions of sleep (18). We wondered whether the sleep induced by activation of dFB$^{23E10\cap 84C10}$ neurons is capable of converting STM to LTM. To test this, we used a 1h courtship training protocol that does not create LTM and activated dFB$^{23E10\cap 84C10}$ neurons optogenetically for 23h following the end of training. LTM was tested 24h after the onset of training (Fig 3A). As seen in Fig 3B, sleep is significantly increased when activating dFB$^{23E10\cap 84C10}$ neurons post-training. As expected, control flies and *dFB-Split>CsChrimson* flies trained for 1h, without increasing sleep post-training, show no LTM (Fig 3C). However, activating dFB$^{23E10\cap 84C10}$ neurons for 23h after a 1h courtship training session led to LTM, as indicated by a significantly higher Suppression Index (Fig 3C). Individual values of courtship indices for untrained and trained males are presented in S16A Fig. These data demonstrate that activation of dFB$^{23E10\cap 84C10}$ neurons following training can convert STM to LTM. An alternative hypothesis is that activation of dFB$^{23E10\cap 84C10}$ neurons promotes LTM consolidation independently of sleep. To rule out this possibility, we sleep-deprived *dFB-Split>CsChrimson* flies following the 1h training session while they were optogenetically activated. This manipulation resulted in sleep loss (Fig 3B) and no LTM (Fig 3C). Thus, we conclude that the sleep that is induced by activation of dFB$^{23E10\cap 84C10}$ neurons can convert STM to LTM.

Silencing dFB$^{23E10\cap 84C10}$ neurons increases sleep and reduces sleep homeostasis

After demonstrating that activation of dFB$^{23E10\cap 84C10}$ neurons increases sleep duration and sleep depth, we performed experiments to silence the activity of these neurons chronically by expressing the hyperpolarizing inward rectifying potassium channel Kir2.1 (52). First, we assessed whether the constitutive expression of Kir2.1 in dFB$^{23E10\cap 84C10}$ neurons leads to anatomical defects. As seen in S17A and S17B Fig, we observed no defects in dFB$^{23E10\cap 84C10}$ neuron numbers or processes when expressing Kir2.1, compared with controls. Surprisingly, total sleep is significantly increased when expressing Kir2.1 in dFB$^{23E10\cap 84C10}$ neurons in female flies (Fig 4A). This effect on sleep is accompanied by an increase of daytime sleep bout duration (Fig 4C) while consolidation at night is unchanged (Fig 4D). These enhancements on sleep are not due to locomotor deficits (Fig 4B). We obtained identical behavioral results when expressing Kir2.1 in dFB$^{23E10\cap 84C10}$ neurons of male flies (S17C-S17F Fig). These results are somewhat surprising as they are similar to the ones obtained when activating dFB$^{23E10\cap 84C10}$ neurons. We thus decided to investigate further. First, we repeated these behavioral experiments using the multibeam system. As seen in Fig 4E, chronic hyperpolarization of dFB$^{23E10\cap 84C10}$ neurons increases total sleep as assessed with DAM5H monitors. Thus, chronic hyperpolarization of dFB$^{23E10\cap 84C10}$ neurons increases sleep and sleep consolidation without disrupting the anatomical properties of these cells. To further investigate the effects of silencing dFB$^{23E10\cap 84C10}$ neurons, we employed an acute silencing approach by expressing Shi^{ts1} (53). Acute silencing (24h, Fig 4F) of dFB$^{23E10\cap 84C10}$ neurons has no effect on sleep in females (Fig 4G) or males (Fig 4H). Altogether, our chronic silencing data further demonstrate that dFB$^{23E10\cap 84C10}$ neurons regulate sleep. However, it is puzzling that both

activation and chronic silencing lead to sleep increases, and that acute silencing has no effect at all.

Multiple studies have suggested a role for dFB neurons in regulating sleep homeostasis. In particular, sleep deprivation increases the excitability of dFB neurons (16) and augmented sleep pressure switches dFB neurons from an electrically silent to an electrically active state (20). Furthermore, reducing the excitability of dFB neurons by reducing levels of the Rho-GTPase-activating protein encoded by the crossveinless-c (cv-c) gene leads to a defect in sleep homeostasis (16). We previously demonstrated that hyperpolarizing all 23E10-GAL4 neurons blocks sleep homeostasis, however this effect was not due to VNC-SP neurons (27). Thus, we concluded that there must be 23E10-GAL4 expressing neurons that are not VNC-SP cells that are involved in sleep homeostasis. We hypothesized that dFB$^{23E10\cap 84C10}$ neurons could be the cells responsible for sleep homeostasis. To test this possibility, we expressed Kir2.1 in dFB$^{23E10\cap 84C10}$ neurons, subjected flies to 12h of mechanical sleep deprivation (SD) during the night and monitored recovery sleep for the subsequent 48h. We observed that control flies show a gradual recovery of lost sleep over the 48h period (Fig 4I). Hyperpolarizing dFB$^{23E10\cap 84C10}$ neurons led to an interesting pattern as *dFB-Split>Kir2.1* flies show some recovery during the first 4-6h following SD, but then did not show additional gains during the remaining recovery period (Fig 4I). To further demonstrate our finding, we quantified sleep recovery after 4h, 6h, 12h, 24h, and 48h. As seen in Fig 4J, sleep recovery is significantly reduced between controls and *dFB-Split>Kir2.1* flies at all time points. However, in *dFB-Split>Kir2.1* flies, sleep recovery at 4h, 6h, 12h, and 24h is significantly different from 0, indicating that these flies show a weaker, but not non-existent, homeostatic rebound (Fig 4J). These data suggest that hyperpolarizing

dFB$^{23E10\cap 84C10}$ neurons does not fully block sleep homeostasis, especially in the immediate period following sleep deprivation. Interestingly, another work showed that hyperpolarizing all 23E10-GAL4 neurons does not impair early (6h) sleep homeostasis (28). In conclusion, our data suggests that there may be multiple groups of neurons involved in sleep homeostasis in the fly brain, with dFB$^{23E10\cap 84C10}$ neurons being an important, but not the sole, player.

dFB$^{23E10\cap 84C10}$ neurons express acetylcholine and glutamate

Previous studies have proposed that dFB neurons are GABAergic (54, 55). However, since these data were obtained using a driver that is not dFB-specific (27), the neurochemical identity of dFB neurons is uncertain. In addition, we showed in our previous work (27) that some 23E10-GAL4 dFB neurons are cholinergic. We thus investigated whether dFB neurons are GABAergic, glutamatergic, or cholinergic by expressing GFP in dFB$^{23E10\cap 84C10}$ neurons and staining them with antibodies to GABA, choline acetyltransferase (ChAT, the enzyme necessary to produce Acetylcholine), and the vesicular glutamate transporter (VGlut). As seen in Fig 5A, we observed no GABA staining in dFB$^{23E10\cap 84C10}$ neurons, but instead found that a minority of these cells express ChAT only or VGlut only, while more than 50% of them express both neurotransmitters (Fig 5B and 5C). Our immunohistochemical analysis thus uncovered that dFB$^{23E10\cap 84C10}$ neurons can be divided in 3 subgroups, neurons that express ChAT and VGlut (ChAT^{+}, VGlut^{+} cells), neurons that express only VGlut (ChAT^{-}, VGlut^{+} cells), and neurons that express only ChAT (ChAT^{+}, VGlut^{-} cells) (Fig 5C right).

To confirm that 23E10-GAL4 dFB neurons are not GABAergic, we expressed GFP using 23E10-GAL4 and stained brains with an antibody to GABA. As seen in S18A Fig, we observed no GABA staining in 23E10-GAL4 dFB neurons. In addition, both a Gad1-AD; 23E10-DBD and

a 84C10-AD; Gad1-DBD Split-GAL4 lines show no expression in dFB neurons (S18B Fig and Fig 5D). Thus, we conclude that dFB$^{23E10\cap 84C10}$ neurons are not GABAergic, contrary to previous reports. To strengthen our findings about the glutamatergic and cholinergic nature of dFB$^{23E10\cap 84C10}$ neurons, we employed a Split-GAL4 strategy using the 84C10 component of dFB-Split paired with neurotransmitter-specific Split elements. An 84C10-AD; ChAT-DBD line expresses in about 16 dFB neurons (ChAT^{+}, VGlut^{+} and ChAT^{+}, VGlut^{-} cells; named dFB$^{ChAT\cap 84C10}$) per brain and no other cells in the brain and VNC (Fig 5E and 5G, S19 and S20 Movies). A VGlut-AD; 84C10-DBD line expresses in 22 dFB cells (ChAT^{+}, VGlut^{+} and ChAT^{-}, VGlut^{+} cells; named dFB$^{VGlut\cap 84C10}$) per brain and shows no other expression in the brain and VNC (Fig 5F and 5G, S21 and S22 Movies). Note that while this manuscript was in preparation, a preprint reported that dFB neurons are glutamatergic and that optogenetic activation of these cells weakly, but significantly, increases sleep (56). However, the Split-GAL4 line used in this study, VGlut-AD; 23E10-DBD may not be dFB-specific, making the interpretation of the behavioral data difficult. We have created two different VGlut-AD; 23E10-DBD lines using the only two VGlut-AD lines known to us. As seen in S18C and S18D Fig and S23 and S24 Movies, both lines express in dFB neurons, but they also express in 8 neurons that are not dFB cells. Note that both independent lines show similar expression in these 8 non-dFB neurons. Thus, our data suggest that VGlut-AD; 23E10-DBD is not a dFB-specific tool and cannot be used to manipulate only dFB neurons. Taken together, our immunostaining data and Split-GAL4 approach indicate that dFB$^{23E10\cap 84C10}$ neurons are not homogenous when it comes to neurochemical identity and can be divided in 3 categories. Considering that acetylcholine is the main excitatory neurotransmitter in the fly system and that glutamate is inhibitory in dFB neurons (56), in

addition to the high level of recurrent connectivity in the dFB (56, 57), it is reasonable to assume that these different categories of dFB$^{23E10\cap 84C10}$ neurons may differentially affect sleep.

To investigate this possibility, we employed optogenetic activation of dFB$^{VGlut\cap 84C10}$ and dFB$^{ChAT\cap 84C10}$ neurons. While these tools are more homogeneous than the dFB-Split line (which contains the 3 populations of dFB neurons), they are not perfect, as both express in 2 of the 3 dFB neurons populations. When we employed our standard optogenetic activation protocol, we saw no effects, perhaps unsurprisingly based on the data obtained when activating all dFB$^{23E10\cap 84C10}$ neurons (S19A Fig). We then increased the frequency of the optogenetic stimulation to 20Hz and found that activating dFB$^{ChAT\cap 84C10}$ neurons significantly increased sleep while no effects were observed with dFB$^{VGlut\cap 84C10}$ cells (S19B Fig). A 50Hz optogenetic activation of dFB$^{ChAT\cap 84C10}$ neurons strongly increases total sleep while it does not with dFB$^{VGlut\cap 84C10}$ neurons (Fig 5H-5K). However, when only examining daytime sleep, we found that a 50Hz activation of dFB$^{VGlut\cap 84C10}$ neurons significantly increases sleep, although significantly less than activation of the cholinergic neurons (Fig 5L). Sleep is not increased during the night when activating dFB$^{VGlut\cap 84C10}$ neurons (S19C Fig). Both daytime and nighttime sleep are increased when activating dFB$^{ChAT\cap 84C10}$ neurons (Fig 5L and S19C Fig). These increases in sleep are not caused by a general deficit in locomotor activity (S19F Fig). These data suggest that within the heterogeneous dFB population, cholinergic neurons play a major role in the sleep-promoting capacity of this region. We obtained similar effects using the multibeam system, ruling out that we have falsely classified periods of micromovements as sleep (S20A-S20D Fig). Further inspection of sleep architecture revealed that while activation of dFB$^{VGlut\cap 84C10}$ neurons increases daytime sleep, it does so by increasing the number of sleep episodes that flies initiate during the day rather than sleep consolidation (S19D and S19E Fig).

During the night, sleep bout numbers are increased, but sleep consolidation is reduced (S19G and S19H Fig). Thus, it appears that activation of dFB$^{VGlut\cap 84C10}$ neurons increases sleep initiation but does not promote sleep consolidation. This is in marked contrast to the activation of dFB$^{ChAT\cap 84C10}$ neurons, which increases sleep consolidation during day and night (S19E and S19H Fig). None of these effects are observed in vehicle-fed controls (S19I-S19M Fig). These data suggest that of dFB$^{VGlut\cap 84C10}$ and dFB$^{ChAT\cap 84C10}$ neurons are likely modulating different aspects of sleep and position dFB$^{ChAT\cap 84C10}$ neurons as the strongest modulators of sleep and sleep consolidation within the dFB.

We then acutely silenced the activity of dFB$^{VGlut\cap 84C10}$ and dFB$^{ChAT\cap 84C10}$ neurons by expressing the thermogenetic Shi^{ts1} actuator. As seen in Fig 5M-5P, silencing either set of dFB neurons significantly reduces sleep, particularly at night. These effects are not due to hyperactivity (Fig 5Q). Altogether, these data confirm that dFB$^{VGlut\cap 84C10}$ and dFB$^{ChAT\cap 84C10}$ neurons regulate sleep.

Finally, we investigated homeostatic sleep in flies in which dFB$^{VGlut\cap 84C10}$ and dFB$^{ChAT\cap 84C10}$ neurons were silenced during the recovery period. As seen in Fig 5R, there were no differences in sleep homeostasis between controls, *VGlut-AD; 84C10-DBD>Shi^{ts1}*, and *84C10-AD; ChAT-DBD>Shi^{ts1}* flies when maintained at 22° post-sleep deprivation. However, raising the temperature to 29° to activate Shi^{ts1} led to an abrogation of sleep rebound in flies with silenced dFB$^{ChAT\cap 84C10}$ neurons while not affecting sleep rebound in flies with silenced dFB$^{VGlut\cap 84C10}$ neurons (Fig 5R).

Cholinergic and glutamatergic signaling in the dFB

To investigate whether cholinergic and glutamatergic transmission plays a role in the sleep modulatory capacity of the dFB, we expressed RNAi constructs against the vesicular glutamate

transporter (VGlut) and the vesicular acetylcholine transporter (VAChT) in dFB$^{VGlut\square 84C10}$ and dFB$^{ChAT\square 84C10}$ neurons. As seen in S21A and S21B Fig, expressing 2 RNAi lines against VACht and 2 RNAi lines against VGlut in dFB$^{VGlut\square 84C10}$ neurons significantly reduces sleep in female flies. These effects are not caused by hyperactivity (S21C Fig). For dFB$^{ChAT\square 84C10}$ neurons, we found that expressing one VAChT RNAi line (27684) or one VGlut RNAi line (40845) significantly increases sleep (S21A and S21B Fig), and that these effects are not due to a locomotor defect (S21C Fig). The second VGlut line (40927) increases sleep during the daytime but it also leads to hypoactivity (S21A-S21C Fig), making conclusions about its use difficult. These data not only suggest that both cholinergic and glutamatergic signaling act in dFB neurons to regulate sleep, but also highlight differences between dFB$^{VGlut\square 84C10}$ and dFB$^{ChAT\square 84C10}$ neurons. Interestingly, a recent preprint reported that reducing VGlut levels in all 23E10-GAL4 expressing neurons reduces sleep (56). However, whether these phenotypes can be attributed to dFB neurons is uncertain.

To investigate whether cholinergic and glutamatergic transmission is necessary for the sleep-promoting capacity of dFB$^{VGlut\square 84C10}$ and dFB$^{ChAT\square 84C10}$ neurons when optogenetically activated, we expressed RNAi constructs against GFP (control), VAChT, and VGlut, while also expressing CsChrimson. As seen in S21D Fig, we found that reducing VAChT or VGlut levels in dFB$^{ChAT\square 84C10}$ neurons does not block the sleep increase observed when using a 50Hz optogenetic activation in female flies. Thus, these data suggest that dFB$^{ChAT\square 84C10}$ neurons use another neuromodulator to promote sleep. For dFB$^{VGlut\square 84C10}$ neurons, we observed no increase in total sleep when expressing GFP RNAi and CsChrimson, in agreement with our findings expressing only CsChrimson (Fig 5K). However, when expressing both VAChT or VGlut RNAi in addition to CsChrimson, we found that a 50Hz optogenetic activation of dFB$^{VGlut\square 84C10}$

neurons significantly increases sleep (S21D Fig). These data suggest that VGlut and VAChT may reduce the sleep-promoting capacity of dFB$^{VGlut\square 84C10}$ neurons and that these cells also use another neuromodulator to increase sleep when sufficiently activated.

Discussion

The strength of the fly model lies in its strong genetic techniques, allowing researchers to selectively manipulate discrete populations of neurons and monitor how specific behaviors are affected. To do so, an impressive collection of binary expression systems have been developed. In particular, the GAL4/UAS system (3) has been the keystone of *Drosophila* neurobiological studies. However, GAL4 drivers are often not specific enough and express in cells outside the region of interest. This can make the task of unequivocally assigning a given behavior to a specific neuron or group of neurons particularly difficult. This lack of specificity can be addressed by employing the intersectional Split-GAL4 technology to refine GAL4 expression (6).

Like mammalian sleep, sleep in *Drosophila* is regulated by multiple areas in the brain (12, 13). An expanding number of studies have suggested a role for dFB neurons in sleep regulation (14-17, 20, 22, 24, 55, 58). The most widely used tool to manipulate dFB neurons is the 23E10-GAL4 driver (20, 21), and thermogenetic or optogenetic activation of 23E10-GAL4 neurons results in increased sleep (18, 24-27). However, we previously demonstrated that 23E10-GAL4 expresses in two cholinergic sleep-promoting neurons located in the VNC (VNC-SP neurons) (27), putting the role of 23E10-GAL4 dFB neurons in question. The involvement of VNC-located neurons in 23E10-GAL4 sleep-promotion has been demonstrated further by a subsequent

paper (28). Simply put, we think that 23E10-GAL4 should no longer be employed as a dFB-specific driver line. Two recent studies, using 23E10-GAL4, suggested that the dFB plays no role at all in sleep (28, 29), a conclusion we did not make based on the finding that there are 23E10-GAL4 expressing neurons involved in sleep homeostasis that are different from VNC-SP neurons (27). However, whether these sleep homeostasis-regulating 23E10-GAL4 neurons are dFB neurons was uncertain. In this study, we sought to unequivocally assess the role of 23E10-GAL4 dFB neurons in sleep regulation.

To do so we adopted a targeted Split-GAL4 strategy combining 20 individual AD lines (selected for the strong dFB expression pattern of their GAL4 counterparts) with a 23E10-DBD line. We screened these 20 novel Split-GAL4 FBS lines behaviorally and anatomically. These experiments identified 7 FBS lines that strongly promote sleep when activated in females and males (S2 Table). In addition, we found 9 lines that moderately modulate at least one sleep parameter (S2 Table). Interestingly, only 4 FBS lines do not change any sleep parameter using both thermogenetic and optogenetic activation protocols (S2 Table). An anatomical assessment of each line revealed that all sleep-promoting FBS lines express in dFB neurons (S1 Table), as expected based on our targeted approach. However, they also express in the metathoracic ganglion of the VNC, especially in the previously described VNC-SP neurons (27). The high frequency of observation of these cells in our FBS lines, and their very typical “bowtie” processes in the brain, suggest that VNC-SP neurons are commonly expressed in many GAL4 lines. In fact, a MultiColor FlpOut (MCFO) study reported that neurons with similar projections (referred to as “sparse T” in this work) are observed in more than 60% of all Janelia GAL4 lines (59). The fact that these “bowtie” neurons are frequently present in many GAL4 lines probably

explains why we see them in the vast majority of our FBS lines (17 out of 20, or 85% of them). This observation also highlights the need to use specific tools when trying to manipulate discrete neurons or groups of neurons. Since VNC-SP neurons are present in many GAL4 lines, it is likely that they are part of the expression pattern of GAL4 lines that have been used to manipulate diverse groups of sleep-modulating neurons. Future studies using GAL4 lines in sleep studies will therefore need to take account of the potential presence of VNC-SP neurons in their expression pattern. Perhaps more importantly, existing data may need to be reinterpreted in light of our findings. Our study also found that the strength of expression within VNC-SP neurons dictates how potent a given FBS line is in promoting sleep. However, the ubiquitous presence of VNC-SP cells in sleep-promoting FBS lines prevented us from unequivocally assessing the role of dFB neurons in sleep regulation using these lines.

Fortunately, we identified a dFB-specific Split-GAL4 line (dFB-Split), which expresses in most 23E10-GAL4 dFB neurons ($dFB^{23E10\cap 84C10}$ neurons). Using either a 1Hz or our standard optogenetic protocol, activation of $dFB^{23E10\cap 84C10}$ neurons does not modulate sleep. However, when we increased the intensity of optogenetic activation (10Hz or above), we found that activating $dFB^{23E10\cap 84C10}$ neurons increases sleep in both males and females. Importantly, we demonstrated this sleep-induction effect using the single beam DAM2 system, the multibeam DAM5H monitor, and by video analysis, ruling out that we have mislabeled periods of micromovements, grooming, or feeding as sleep. In addition, the state induced by activation of $dFB^{23E10\cap 84C10}$ neurons consolidates LTM (see below), suggesting that this state is indeed sleep. Finally, we showed that activation of $dFB^{23E10\cap 84C10}$ neurons increases arousal threshold, indicating that flies sleep deeper when $dFB^{23E10\cap 84C10}$ neurons are activated. Crucially, though

the sleep obtained by dFB$^{23E10\cap 84C10}$ neurons activation is deeper, it is reversible, which is an important hallmark of sleep.

Chronic hyperpolarization of dFB$^{23E10\cap 84C10}$ neurons interferes with sleep homeostasis. We found that expressing Kir2.1 in dFB$^{23E10\cap 84C10}$ neurons leads to a reduction in the amount of sleep that flies recover following sleep deprivation, when compared with controls. However, *dFB-Split>Kir2.1* flies show a modest, but significant sleep rebound, especially during the first hours in the recovery period. Interestingly, a recent study found that hyperpolarizing all 23E10-GAL4 neurons does not impair early (6h) sleep homeostasis (28). These data demonstrate that dFB$^{23E10\cap 84C10}$ neurons are involved in sleep homeostasis but indicate that there are other sleep homeostasis-regulating neurons in the fly nervous system, a suggestion also made by others (60). Surprisingly, chronic silencing of dFB$^{23E10\cap 84C10}$ neurons increases sleep, confirming that dFB neurons modulate sleep. This effect is not caused by gross morphological defects created by the expression of Kir2.1 throughout the development and life of the flies. How do we explain this result? dFB neurons have been mostly implicated in sleep homeostasis. To be efficient at inducing sleep only in response to sleep pressure, the activity of the underlying neuronal system must be tightly regulated. This is the case for dFB neurons, which are subject to strong dopaminergic regulation (15, 17, 20, 45) and are highly interconnected (56, 57). Additionally, dFB$^{23E10\cap 84C10}$ neurons are neurochemically heterogeneous (see below), containing 3 different groups of neurons based on their expression of glutamate and acetylcholine. Acetylcholine is the main excitatory neurotransmitter in the fly nervous system, while glutamate acts as an inhibitory neurotransmitter in dFB neurons (56). Thus, the dFB is a highly interconnected network containing excitatory and inhibitory connections that is under strong dopaminergic inhibition

under baseline conditions. This organization probably ensures stability within the dFB network, to regulate its activity in response to increasing sleep pressure effectively. We hypothesize that chronic hyperpolarization of all dFB$^{23E10\cap 84C10}$ neurons disrupts the balance of inhibitory and excitatory connections within the dFB. This may lead to complex effects on the activity of individual cells in this heterogeneous population, generating unexpected and complicated sleep phenotypes. Using neurotransmitter- and dFB-specific Split-GAL4 lines to acutely activate or silence more homogeneous populations of dFB neurons led to sleep increases and sleep decreases, respectively.

Why do dFB$^{23E10\cap 84C10}$ neurons require such a strong activation protocol to increase sleep? Considering that dFB neurons are subject to dopaminergic regulation (15, 17, 20, 45), we hypothesize that under baseline conditions, dFB neurons are under severe dopaminergic inhibition and that our standard optogenetic activation protocol is not sufficient to bring these cells above firing threshold. Increasing the intensity of the activation protocol reliably leads to sleep increases in what appears to be a direct relationship. Importantly, following 12h of sleep-deprivation, individual dFB neurons increase their firing frequencies, with some neurons capable of firing up to 50Hz (16). These data indicate that our optogenetic protocols, using 10Hz, 20Hz, and 50Hz frequencies to activate dFB neurons, are within the physiological range of normal firing properties for these cells.

A recent preprint showed that optogenetic activation of dFB neurons, as labelled with a VGlut-AD; 23E10-DBD line, increased sleep when using an activation protocol consisting of 10 bursts of LED ON compressed in one half of a 500:500 ms duty cycle. Interestingly, a 10Hz activation,

delivering the same number of light pulses spread evenly across time failed to increase sleep (56). The authors thus concluded that the temporal structure of the activation protocol used to activate dFB neurons is important to their sleep-promoting capacities (56). Using our dFB-specific tool we show that using optogenetic activations of 10Hz or more lead to significant increases in sleep. Thus, we propose a simpler model, in which the intensity of the activation protocol dictates whether or not dFB neurons promote sleep when activated. While we expect that the expression pattern of our dFB-Split driver and the VGlut-AD; 23E10-DBD line contains mostly similar neurons (since they both rely on 23E10-DBD), we show in this study that they are not fully identical. Our analysis, using two independent VGlut-AD; 23E10-DBD lines, shows that while both lines express in many dFB neurons, they also express in 8 additional non-dFB neurons. Thus, VGlut-AD; 23E10-DBD is not a suitable tool to assess the role of the dFB in sleep regulation, as it is not a dFB-specific driver line. We hypothesize that these differences in expression pattern probably explain the difference between our results and others (56).

Previous work showed that dFB neurons are heterogeneous (16) and proposed that these neurons are GABAergic (54, 55). Our work, using both Split-GAL4 and immunocytochemistry approaches, reveals that dFB neurons are not GABAergic. We believe that the mischaracterization of dFB neurons as GABAergic is a consequence of using a non-dFB-specific tool, 23E10-GAL4. This finding further reinforces the need to use specific tools when trying to decipher the neural circuitries underlying complex behaviors.

In this study, we found that most $dFB^{23E10\cap 84C10}$ neurons express both glutamate and acetylcholine, while a minority of them only express one of these two neurotransmitters. Thus, $dFB^{23E10\cap 84C10}$ neurons can be divided into 3 subgroups: $ChAT^{+}$, $VGlut^{+}$ cells; $ChAT^{-}$, $VGlut^{+}$

cells; and ChAT^{+}, VGlut^{-} cells. Using neurotransmitter- and dFB-specific tools, our behavioral data support a major role in sleep promotion and sleep homeostasis for the cholinergic dFB$^{ChAT\square 84C10}$ neurons, which consist of 2 of the 3 dFB subgroups. Activating glutamatergic dFB$^{VGlut\square 84C10}$ neurons has a much milder effect on sleep, only increasing sleep during the day. When examining sleep architecture, we found that dFB$^{ChAT\square 84C10}$ neurons increase sleep consolidation when activated, while dFB$^{VGlut\square 84C10}$ cells do not. We note that activation of VGlut-AD; 23E10-DBD expressing neurons also led to a modest sleep increase during the day (56), however, since this driver is not dFB-specific, the cellular origin of this sleep increase is uncertain. Acute silencing of either dFB$^{VGlut\square 84C10}$ or dFB$^{ChAT\square 84C10}$ neurons reduces sleep, further demonstrating that dFB neurons regulate sleep.

Our RNAi analysis revealed that dFB neurons rely on cholinergic and glutamatergic signaling to modulate sleep, as reducing levels of VGlut or VAChT in dFB$^{VGlut\square 84C10}$ and dFB$^{ChAT\square 84C10}$ neurons modulates sleep in opposite directions. These RNAi data further support that dFB neurons regulate sleep but may be difficult to interpret, as these manipulations are targeting 2 of the 3 dFB subgroups. For example, expressing VGlut RNAi in dFB$^{VGlut\square 84C10}$ neurons affects the ChAT^{+}, VGlut^{+} cells and ChAT^{-}, VGlut^{+} cells, but expressing VAChT RNAi should only affect the ChAT^{+}, VGlut^{+} neurons. When considering the high level of interconnectivity within the dFB (56, 57), predicting the sleep effect of RNAi expression in multiple subgroups of dFB neurons may be difficult. This means that further dissection of the dFB circuitry is required to fully elucidate how this neuronal population functions. Nevertheless, we hypothesize that reducing the levels of VGlut or VAChT in different groups of dFB neurons disrupts the balance of excitatory and inhibitory connections within the dFB, mitigating its stability, and leading to sleep phenotypes under baseline conditions.

Our RNAi analysis also shows that in addition to cholinergic and glutamatergic signaling, dFB neurons probably use another neuromodulator to increase sleep when activated. We suspect that dFB neurons use neuropeptidergic transmission to increase sleep. In fact, a previous study proposed that dFB neurons express the Allatostatin-A (AstA) neuropeptide (55), the fly homolog of galanin, an important sleep-regulating peptide in the mammalian brain (61). However, a second study claims that there is no AstA expression in the dFB (28). Whether AstA or another neuropeptide regulates the sleep-promoting capacity of dFB$^{VGlut\cap 84C10}$ and dFB$^{ChAT\cap 84C10}$ neurons requires further studies. Taken together, these data indicate that additional genetic dissection and studies of individual dFB neurons will be needed to fully understand the contribution of neurochemically distinct dFB neurons to sleep regulation.

Finally, a previous study demonstrated that vFB neurons regulate learning-dependent sleep and that these cells play an essential role in LTM consolidation (18). The same work proposed that vFB and dFB neurons promote different types of sleep that may underlie different functions (18). While vFB and dFB neurons may promote sleep in response to different drives, a learning-dependent sleep drive for vFB neurons and a homeostatic sleep drive for dFB cells, we found that the sleep obtained by activation of dFB$^{23E10\cap 84C10}$ neurons can consolidate LTM. Thus, we conclude that the benefit of sleep on memory consolidation is not circuit specific.

In conclusion, our work demonstrates that the dFB is neurochemically heterogeneous and that these neurons modulate sleep, especially sleep homeostasis. In addition, dFB-generated sleep can consolidate LTM. Further work is needed to dissect the heterogeneous dFB population and will identify the connectivity and contribution of individual dFB neurons in sleep regulation.

Materials and Methods

Drosophila stocks and rearing

Flies were cultured at 25˚C with 50% humidity under a 12h light:12h dark cycle. Flies were kept on a standard yeast and molasses diet (per 1L: 50g yeast, 15g sucrose, 28g corn syrup, 33.3mL molasses, 9g agar). Fly stocks used in this study are listed in S3 Table.

Sleep behavioral experiments

Sleep was assessed as previously described (11, 19, 27). 4-10 day old virgin females or males were used as described in figure legends. Briefly, flies were placed into individual 65 mm tubes and all activity was continuously measured through the Trikinetics Drosophila Activity Monitoring System (DAM2, www.Trikinetics.com, Waltham, Ma). Locomotor activity was measured in 1-minute bins and sleep was defined as periods of quiescence lasting at least 5 minutes. For multibeam monitoring, we used the DAM5H monitors (www.Trikinetics.com, Waltham, Ma).

Multibeam system validation: paired MB and video analysis

To validate the accuracy and sensitivity of the Trikinetics DAM5H multibeam system, Cs flies were placed into individual 65 mm tubes and monitored by the DAM5H system while simultaneously being video recorded. The multibeam system was set to record moves (fly

movement from one beam to another), counts (fly movement within a beam), and position in the tube. Flies were monitored and recorded for 10 minutes. The multibeam data was measured in 1-minute bins and each minute was scored based on highest activity level that occurred in that minute: moves, counts, and rest. A 1-minute bin that had moves was scored as moves. A 1-minute bin that had counts, but no moves, was scored as micromovements. A 1-minute bin that had neither moves nor counts was scored as rest. The videos were manually analyzed for fly behaviors that all fell into the different movement categories of moves (walking), micromovements (feeding, grooming, proboscis extension, posture change, single leg movement), and rest. These behaviors were scored in the same 1-minute bins to compare directly with multibeam detection. Sensitivity and accuracy of the multibeam were calculated by the following formulas,

Sensitivity = minutes with a behavior identified by the multibeam system / all visually labeled minutes of the same behavior

Accuracy = correctly identified minutes with a behavior by the multibeam system to / all identified minutes with the same behavior by the multibeam system

Multibeam and video analysis of optogenetic activation of control and dFB-Split flies

For Fig 2P, flies expressing CsChrimson were loaded into individual 65mm tubes with food supplemented with 400µM all-trans retinal and monitored by the DAM5H system while simultaneously being video recorded. The multibeam system was set to record moves (fly movement from one beam to another), counts (fly movement within a beam), and position in the tube. Flies were monitored and recorded for 10 minutes of baseline activity with LEDs OFF

followed immediately by 10 minutes of activation with LEDs ON at 20Hz. Multibeam data and video analysis was performed in the same manner as for multibeam validation with CS flies.

Quantitative Video analysis

For Fig 2Q, video recording was performed as previously described (27). Flies fed food supplemented with 400µM all-trans retinal (Sigma, #R2500) or vehicle were loaded into individual 65mm tubes and placed on custom-built platforms. One webcam for 2 platforms was used to record the flies for 30 minutes starting at ZT1 (one hour after lights turn on in the morning). Fly behavior was manually scored and categorized as walking, grooming, feeding, resting (inactivity < 5min), or sleeping (inactivity > 5min). Videos were recorded on consecutive days for baseline (LED OFF) and activation (LED ON). Three separate experiments were performed, and the pooled data is shown.

Optogenetic activation

For optogenetic activation, flies expressing CsChrimson were loaded into individual 65mm tubes with food supplemented with 400µM all-trans retinal (Sigma, #R2500) or vehicle control and kept under 12h low-light/12h darkness conditions for 48h. Sleep was then monitored for 24h of baseline measurements. To activate CsChrimson, flies were put under 627nm LEDs (LuxeonStar LXM2-PD01-0040) and set to different activation protocols. The standard intensity protocol is set to a pulse cycle of (5ms on, 95ms off) x 20 with a 4 second delay between pulse cycles. The light intensity of this protocol is 0.078mW/mm^2. For the 1Hz protocol a cycle of 5ms on, 995ms off flashing continuously was used (light intensity=0.05mW/mm^2). For the 10Hz protocol a cycle of 5ms on, 95ms off flashing continuously was used (light intensity=0.078mW/mm^2). For

the 20Hz protocol a cycle of 5ms on, 45ms off flashing continuously was used (light intensity=0.118mW/mm^2). For 50Hz, a cycle of 5ms on, 15ms off flashing continuously was used (light intensity=0.252mW/mm^2). The light intensity of the LED constantly ON protocol is 0.565mW/mm^2. A photodiode sensor (S120C, Thorlabs) paired with a digital console (PM100D, Thorlabs) was used to measure light intensity.

Sleep deprivation assay

Sleep deprivation was performed as previously described (19, 27, 62, 63). Briefly, flies were placed into individual 65 mm tubes and the sleep-nullifying apparatus (SNAP) was used to sleep deprive flies for 12 hours during the dark phase. For Fig 4J, sleep homeostasis was calculated for each individual fly as the ratio of the minutes of sleep gained above baseline after 4h, 6h, 12h, 24h, and48h of recovery sleep divided by the total min of sleep lost during 12h of sleep deprivation. For Fig 5R, flies were maintained at 22° during baseline and sleep deprivation. Following 12h of sleep deprivation, a group of flies was maintained at 22° during recovery while another one was transferred to 29° to activate Shi^{ts1}. Sleep homeostasis was calculated for each individual fly as the ratio of the minutes of sleep gained above baseline during 24h of recovery sleep divided by the total min of sleep lost during 12h of sleep deprivation.

Arousal threshold

Arousal threshold was measured on flies that were optogenetically activated. Control flies and flies expressing CsChrimson were loaded into individual 65mm glass tubes containing food supplemented with 400 μM all-trans retinal (Sigma, #R2500) or vehicle control. After 3 days the tubes were placed onto custom 3D printed trays, 16 tubes per tray. Video of two trays was

recorded using a Raspberry Pi NoIR camera. Arousal stimulus was provided by three coreless vibration motors (7x25mm) capable of 8,000-16,000rmp vibration. Vibration pattern and intensity were controlled by a DRV2605 haptic controller (Adafruit) paired with a Raspberry Pi 3 Model B+. A custom program was written in python to control the video and motor vibration. The programmed sequence starts with turning video recording on. Ten minutes after recording starts the stimulus pattern begins. The DRV2605 vibration effect used is transition click (effects 62 to 58) starting at 20% intensity and increasing in 20% increments to 100% intensity. Vibration occurred for 200ms followed by 800ms no vibration repeating four times followed by a 15sec break before the next increasing stimulus starts. Video recording continued for 10 minutes after final vibration stimulus. This program repeated once per hour from ZT3 to ZT9. Videos were manually scored. Flies inactive during the 5 minutes directly before the stimulus began were scored as sleeping. Sleeping flies were then assessed for movement during the increasing intensity stimulus. Arousal was reported based on the percentage of flies moving at each vibration intensity. Arousal threshold was scored on consecutive days for baseline (LED OFF) and activation (LED ON). The code for the arousal threshold can be found at https://github.com/mcellinj/Dissel-lab-arousal-apparatus

Immunocytochemistry

Flies were cold anesthetized, brains and VNC were dissected in ice cold Schneider's Drosophila Medium (Gibco, 21720024), and blocked in 5% normal goat serum. Following blocking, flies were incubated overnight at 4˚C in primary antibody, washed in PBST, and incubated overnight at 4˚C in secondary antibody. Primary antibodies used were chicken anti-GFP (1:1000; Aves Labs, Inc, #GFP-1020), mouse anti-bruchpilot (1:50; Developmental Studies Hybridoma Bank

(DSHB), nc82-s), mouse anti-ChAT (1:100; DSHB, Chat4b1-c), rabbit anti-vGlut (1:500; DiAntonio lab (64), Washington University), and rabbit anti-GABA (1:1000; Sigma-Aldrich, #A2052). Secondary antibodies used were goat anti-chicken AlexaFluor 488 (1:800; Invitrogen, #A32931), goat anti-mouse AlexaFluor 555 (1:400; Invitrogen #A32727), goat anti-rabbit AlexaFluor 555 (1:400; Invitrogen, #A32732), goat anti-mouse AlexaFluor 633 (1:400; Invitrogen, $A21052), and goat anti-rabbit AlexaFluor 633 (1:400; Invitrogen, #A21071). Brains and VNCs were mounted on polylysine-treated slides in Vectashield H-1000 mounting medium. Imaging was performed on a Zeiss 510 meta confocal microscope using a Plan-Apochromat 20x or Plan-Neofluar 40x objective. Z-series images were acquired with a 1 µm slice size using the same settings (laser power, gain, offset) to allow for comparison across genotypes. Images were processed and analyzed using ImageJ.

For non-CNS adult tissues (wings, legs, ovaries, and guts). Flies were collected, fixed, and stained similarly as brains and VNCs but following incubation with secondary antibodies and washing 3 times with PBST, tissue was incubated with 10µM 4',6-Diamidino-2-Phenylindole, Dihydrochloride (DAPI) (Invitrogen D1306) for 15 minutes at room temperature. Tissues were then washed in PBST and mounted in Vectashield.

GFP-DD

For destabilized GFP (GFP-DD) experiments, flies expressing GFP-DD were maintained on standard food. Flies were transferred to food containing 1mM Trimethoprim (TMP) solution (T1225, Teknova) or DMSO as control. Following 24 hours on TMP or DMSO containing food, flies were cold anesthetized and brains and VNCs were dissected. Brains and VNCs were fixed in 4% paraformaldehyde, washed in PBST, and mounted on slides. Brains and VNCs were

imaged on a Zeiss 510 meta confocal microscope using a Plan-Neofluar 40X objective. GFP intensity was measured in ImageJ.

Courtship Conditioning Protocol

Naïve males were collected upon eclosion and isolated into glass sleep tubes. 48+ hours prior to training, males were transferred into new glass sleep tubes containing either vehicle or all-trans retinal dissolved in food and loaded into monitors. The 24h period prior to training served as the baseline sleep measurement. Naïve males were transferred into 13 mm x 100 mm glass culture tubes with food at the bottom, with respective vehicle or all-trans retinal additions, and paired for 1h with a mated trainer female (trained group) or alone (untrained group). Males were then transferred back into sleep tubes on the respective diet and sleep was monitored for the 23h post-training period. Flies subjected to LED activation were placed under 627 nm LED light at 20 Hz (5 ms ON and 45 ms OFF continuous cycles) for the post-training period. The sleep deprived group experienced LED activation and sleep deprivation over the 23h post-training period using the SNAP (19, 27, 62, 63). 24h after the onset of training, male flies were placed into courtship chambers with a mated tester female and video recorded for the 10 minute testing period. The courtship index (CI) was calculated using CI = (Time Spent on Courtship Behaviors / Total Time of Test) * 100. The suppression index (SI) was then calculated using SI = 100 * (1 – (CI Trained / CI Untrained)). Trainer and tester female mating status was visually confirmed after *don juan*-GFP pairing prior to training.

Courtship Video Processing and Scoring

Courtship videos were recorded for 10 minutes at 20 fps through OBS Studio software. Videos were analyzed using FlyTracker software (65, 66) and outputs were saved as JAABA files. The visualization tool within FlyTracker was used to confirm the assignment of male and female flies and any switches in labeling were corrected using this feature. The videos and corresponding output files were scored using JAABA, a MATLAB-based machine learning program (67). Positive and negative frame examples were used to train three different scoring classifiers: OriChase (includes orientation and chase), SingWing (singing and wing extension), and MountCop (includes mounting and copulation). The accuracy of these classifiers was verified by built-in ground truth data and comparison to hand-scored tests. JAABAPlot was used to output the CI for each male fly and the resulting SI was calculated from these values.

Statistical analysis

Statistical analyses were performed with Prism10 software (GraphPad). Normal distribution was assessed with the D'Agostino-Pearson test. Normally distributed data were analyzed with parametric statistics: t-test, one-way analysis of variance or two-way ANOVA followed by the planned pairwise multiple comparisons as described in the legends. For data that significantly differed from the normal distribution, non-parametric statistics were applied, including Mann-Whitney U test, Kruskal–Wallis test followed by Dunn's multiple test, and Wilcoxon signed-rank test. Some non-normally distributed data were subjected to log transformation or Box-Cox transformation before two-way ANOVA followed by planned pairwise multiple comparisons as described in the legends. When box plots are used, the bottom and top of each box represents the first and third quartile, and the horizontal line dividing the box is the median. The whiskers

represent the 10th and 90th percentiles. All statistically different groups are defined as *P < 0.05, **P<0.01, ***P<0.001 and ****P<0.0001.

Acknowledgments: We thank Aaron DiAntonio, Kausik Si, Gerry Rubin, and Paul Shaw for sharing reagents and protocols.

Reference and Notes:

1. Park HG, Carmel JB. Selective Manipulation of Neural Circuits. Neurotherapeutics. 2016;13(2):311-24.
2. Moulin TC, Covill LE, Itskov PM, Williams MJ, Schioth HB. Rodent and fly models in behavioral neuroscience: An evaluation of methodological advances, comparative research, and future perspectives. Neurosci Biobehav Rev. 2021;120:1-12.
3. Brand AH, Perrimon N. Targeted gene expression as a means of altering cell fates and generating dominant phenotypes. Development. 1993;118(2):401-15.
4. Lai SL, Lee T. Genetic mosaic with dual binary transcriptional systems in Drosophila. Nat Neurosci. 2006;9(5):703-9.
5. Potter CJ, Tasic B, Russler EV, Liang L, Luo L. The Q system: a repressible binary system for transgene expression, lineage tracing, and mosaic analysis. Cell. 2010;141(3):536-48.
6. Luan H, Peabody NC, Vinson CR, White BH. Refined spatial manipulation of neuronal function by combinatorial restriction of transgene expression. Neuron. 2006;52(3):425-36.
7. Keene AC, Duboue ER. The origins and evolution of sleep. J Exp Biol. 2018;221(Pt 11).
8. Miyazaki S, Liu CY, Hayashi Y. Sleep in vertebrate and invertebrate animals, and insights into the function and evolution of sleep. Neurosci Res. 2017;118:3-12.
9. Borbely AA. A two process model of sleep regulation. Hum Neurobiol. 1982;1(3):195-204.
10. Hendricks JC, Finn SM, Panckeri KA, Chavkin J, Williams JA, Sehgal A, et al. Rest in Drosophila is a sleep-like state. Neuron. 2000;25(1):129-38.
11. Shaw PJ, Cirelli C, Greenspan RJ, Tononi G. Correlates of sleep and waking in Drosophila melanogaster. Science. 2000;287(5459):1834-7.
12. Shafer OT, Keene AC. The Regulation of Drosophila Sleep. Curr Biol. 2021;31(1):R38-R49.
13. Dissel S. Drosophila as a Model to Study the Relationship Between Sleep, Plasticity, and Memory. Front Physiol. 2020;11:533.
14. Donlea JM, Thimgan MS, Suzuki Y, Gottschalk L, Shaw PJ. Inducing sleep by remote control facilitates memory consolidation in Drosophila. Science. 2011;332(6037):1571-6.
15. Ueno T, Tomita J, Tanimoto H, Endo K, Ito K, Kume S, et al. Identification of a dopamine pathway that regulates sleep and arousal in Drosophila. Nat Neurosci. 2012;15(11):1516-23.
16. Donlea JM, Pimentel D, Miesenbock G. Neuronal Machinery of Sleep Homeostasis in Drosophila. Neuron. 2014;81(6):1442.

1037 17. Liu Q, Liu S, Kodama L, Driscoll MR, Wu MN. Two dopaminergic neurons signal to the dorsal fan-
1038 shaped body to promote wakefulness in Drosophila. Curr Biol. 2012;22(22):2114-23.
1039 18. Dag U, Lei Z, Le JQ, Wong A, Bushey D, Keleman K. Neuronal reactivation during post-learning
1040 sleep consolidates long-term memory in Drosophila. Elife. 2019;8.
1041 19. Dissel S, Angadi V, Kirszenblat L, Suzuki Y, Donlea J, Klose M, et al. Sleep restores behavioral
1042 plasticity to Drosophila mutants. Curr Biol. 2015;25(10):1270-81.
1043 20. Pimentel D, Donlea JM, Talbot CB, Song SM, Thurston AJF, Miesenbock G. Operation of a
1044 homeostatic sleep switch. Nature. 2016;536(7616):333-7.
1045 21. Jenett A, Rubin GM, Ngo TT, Shepherd D, Murphy C, Dionne H, et al. A GAL4-driver line resource
1046 for Drosophila neurobiology. Cell Rep. 2012;2(4):991-1001.
1047 22. Kempf A, Song SM, Talbot CB, Miesenbock G. A potassium channel beta-subunit couples
1048 mitochondrial electron transport to sleep. Nature. 2019;568(7751):230-4.
1049 23. Alam MA, Kumar S, McGinty D, Alam MN, Szymusiak R. Neuronal activity in the preoptic
1050 hypothalamus during sleep deprivation and recovery sleep. J Neurophysiol. 2014;111(2):287-99.
1051 24. Qian Y, Cao Y, Deng B, Yang G, Li J, Xu R, et al. Sleep homeostasis regulated by 5HT2b receptor in
1052 a small subset of neurons in the dorsal fan-shaped body of drosophila. Elife. 2017;6.
1053 25. Yap MHW, Grabowska MJ, Rohrscheib C, Jeans R, Troup M, Paulk AC, et al. Oscillatory brain
1054 activity in spontaneous and induced sleep stages in flies. Nat Commun. 2017;8(1):1815.
1055 26. Berry JA, Cervantes-Sandoval I, Chakraborty M, Davis RL. Sleep Facilitates Memory by Blocking
1056 Dopamine Neuron-Mediated Forgetting. Cell. 2015;161(7):1656-67.
1057 27. Jones JD, Holder BL, Eiken KR, Vogt A, Velarde AI, Elder AJ, et al. Regulation of sleep by
1058 cholinergic neurons located outside the central brain in Drosophila. PLoS Biol. 2023;21(3):e3002012.
1059 28. De J, Wu M, Lambatan V, Hua Y, Joiner WJ. Re-examining the role of the dorsal fan-shaped body
1060 in promoting sleep in Drosophila. Curr Biol. 2023;33(17):3660-8 e4.
1061 29. Keleş MF, Sapci AOB, Brody C, Palmer I, Le C, Taştan Ö, et al. FlyVISTA, an Integrated Machine
1062 Learning Platform for Deep Phenotyping of Sleep in Drosophila. bioRxiv.
1063 2024:2023.10.30.564733.
1064 30. Tirian L, Dickson BJ. The VT GAL4, LexA, and split-GAL4 driver line collections for targeted
1065 expression in the *Drosophila* nervous system. BioRxiv 198648 [Preprint] October 5, 2017 Available from:
1066 https://doiorg/101101/198648. 2017.
1067 31. Dionne H, Hibbard KL, Cavallaro A, Kao JC, Rubin GM. Genetic Reagents for Making Split-GAL4
1068 Lines in Drosophila. Genetics. 2018;209(1):31-5.
1069 32. Hamada FN, Rosenzweig M, Kang K, Pulver SR, Ghezzi A, Jegla TJ, et al. An internal thermal
1070 sensor controlling temperature preference in Drosophila. Nature. 2008;454(7201):217-20.
1071 33. Klapoetke NC, Murata Y, Kim SS, Pulver SR, Birdsey-Benson A, Cho YK, et al. Independent optical
1072 excitation of distinct neural populations. Nat Methods. 2014;11(3):338-46.
1073 34. van Alphen B, Yap MH, Kirszenblat L, Kottler B, van Swinderen B. A dynamic deep sleep stage in
1074 Drosophila. J Neurosci. 2013;33(16):6917-27.
1075 35. Ishimoto H, Lark A, Kitamoto T. Factors that Differentially Affect Daytime and Nighttime Sleep in
1076 Drosophila melanogaster. Front Neurol. 2012;3:24.
1077 36. Lamaze A, Ozturk-Colak A, Fischer R, Peschel N, Koh K, Jepson JE. Regulation of sleep plasticity
1078 by a thermo-sensitive circuit in Drosophila. Sci Rep. 2017;7:40304.
1079 37. Parisky KM, Agosto Rivera JL, Donelson NC, Kotecha S, Griffith LC. Reorganization of Sleep by
1080 Temperature in Drosophila Requires Light, the Homeostat, and the Circadian Clock. Curr Biol.
1081 2016;26(7):882-92.
1082 38. Kim JH, Ki Y, Lee H, Hur MS, Baik B, Hur JH, et al. The voltage-gated potassium channel Shaker
1083 promotes sleep via thermosensitive GABA transmission. Commun Biol. 2020;3(1):174.

1084 39. Isaac RE, Li C, Leedale AE, Shirras AD. Drosophila male sex peptide inhibits siesta sleep and
1085 promotes locomotor activity in the post-mated female. Proc Biol Sci. 2010;277(1678):65-70.
1086 40. Khericha M, Kolenchery JB, Tauber E. Neural and non-neural contributions to sexual dimorphism
1087 of mid-day sleep in Drosophila melanogaster: a pilot study. Physiol Entomol. 2016;41(4):327-34.
1088 41. Wu B, Ma L, Zhang E, Du J, Liu S, Price J, et al. Sexual dimorphism of sleep regulated by juvenile
1089 hormone signaling in Drosophila. PLoS Genet. 2018;14(4):e1007318.
1090 42. Kim H, Kirkhart C, Scott K. Long-range projection neurons in the taste circuit of Drosophila. Elife.
1091 2017;6.
1092 43. Dolan MJ, Luan H, Shropshire WC, Sutcliffe B, Cocanougher B, Scott RL, et al. Facilitating Neuron-
1093 Specific Genetic Manipulations in Drosophila melanogaster Using a Split GAL4 Repressor. Genetics.
1094 2017;206(2):775-84.
1095 44. Sethi S, Wang JW. A versatile genetic tool for post-translational control of gene expression in
1096 Drosophila melanogaster. Elife. 2017;6.
1097 45. Dissel S, Klose MK, van Swinderen B, Cao L, Ford M, Periandri EM, et al. Sleep-promoting
1098 neurons remodel their response properties to calibrate sleep drive with environmental demands. PLoS
1099 Biol. 2022;20(9):e3001797.
1100 46. French AS, Geissmann Q, Beckwith EJ, Gilestro GF. Sensory processing during sleep in Drosophila
1101 melanogaster. Nature. 2021;598(7881):479-82.
1102 47. van Alphen B, Semenza ER, Yap M, van Swinderen B, Allada R. A deep sleep stage in Drosophila
1103 with a functional role in waste clearance. Sci Adv. 2021;7(4).
1104 48. Goel N, Rao H, Durmer JS, Dinges DF. Neurocognitive consequences of sleep deprivation. Semin
1105 Neurol. 2009;29(4):320-39.
1106 49. Diekelmann S, Born J. The memory function of sleep. Nat Rev Neurosci. 2010;11(2):114-26.
1107 50. Denis D, Cairney SA. Neural reactivation during human sleep. Emerg Top Life Sci. 2023;7(5):487-
1108 98.
1109 51. Lei Z, Henderson K, Keleman K. A neural circuit linking learning and sleep in Drosophila long-
1110 term memory. Nat Commun. 2022;13(1):609.
1111 52. Baines RA, Uhler JP, Thompson A, Sweeney ST, Bate M. Altered electrical properties in
1112 Drosophila neurons developing without synaptic transmission. J Neurosci. 2001;21(5):1523-31.
1113 53. Kitamoto T. Conditional modification of behavior in Drosophila by targeted expression of a
1114 temperature-sensitive shibire allele in defined neurons. J Neurobiol. 2001;47(2):81-92.
1115 54. Ni JD, Gurav AS, Liu W, Ogunmowo TH, Hackbart H, Elsheikh A, et al. Differential regulation of
1116 the Drosophila sleep homeostat by circadian and arousal inputs. Elife. 2019;8.
1117 55. Donlea JM, Pimentel D, Talbot CB, Kempf A, Omoto JJ, Hartenstein V, et al. Recurrent Circuitry
1118 for Balancing Sleep Need and Sleep. Neuron. 2018;97(2):378-89 e4.
1119 56. Hasenhuetl PS, Sarnataro R, Vrontou E, Rorsman HO, Talbot CB, Brain R, et al. A half-centre
1120 oscillator encodes sleep pressure. bioRxiv. 2024:2024.02.23.581780.
1121 57. Hulse BK, Haberkern H, Franconville R, Turner-Evans DB, Takemura SY, Wolff T, et al. A
1122 connectome of the Drosophila central complex reveals network motifs suitable for flexible navigation
1123 and context-dependent action selection. Elife. 2021;10.
1124 58. Tainton-Heap LAL, Kirszenblat LC, Notaras ET, Grabowska MJ, Jeans R, Feng K, et al. A
1125 Paradoxical Kind of Sleep in Drosophila melanogaster. Curr Biol. 2021;31(3):578-90 e6.
1126 59. Meissner GW, Nern A, Dorman Z, DePasquale GM, Forster K, Gibney T, et al. A searchable image
1127 resource of Drosophila GAL4 driver expression patterns with single neuron resolution. Elife. 2023;12.
1128 60. Satterfield LK, De J, Wu M, Qiu T, Joiner WJ. Inputs to the sleep homeostat originate outside the
1129 brain. J Neurosci. 2022.

61. Sherin JE, Elmquist JK, Torrealba F, Saper CB. Innervation of histaminergic tuberomammillary neurons by GABAergic and galaninergic neurons in the ventrolateral preoptic nucleus of the rat. J Neurosci. 1998;18(12):4705-21.
62. Seugnet L, Suzuki Y, Vine L, Gottschalk L, Shaw PJ. D1 receptor activation in the mushroom bodies rescues sleep-loss-induced learning impairments in Drosophila. Curr Biol. 2008;18(15):1110-7.
63. Melnattur K, Morgan E, Duong V, Kalra A, Shaw PJ. The Sleep Nullifying Apparatus: A Highly Efficient Method of Sleep Depriving Drosophila. J Vis Exp. 2020(166).
64. Daniels RW, Collins CA, Chen K, Gelfand MV, Featherstone DE, DiAntonio A. A single vesicular glutamate transporter is sufficient to fill a synaptic vesicle. Neuron. 2006;49(1):11-6.
65. Barbaro BA, Lukacsovich T, Agrawal N, Burke J, Bornemann DJ, Purcell JM, et al. Comparative study of naturally occurring huntingtin fragments in Drosophila points to exon 1 as the most pathogenic species in Huntington's disease. Hum Mol Genet. 2015;24(4):913-25.
66. Barwell T, Raina S, Seroude L. Versatile method to measure locomotion in adult Drosophila. Genome. 2021;64(2):139-45.
67. Kabra M, Robie AA, Rivera-Alba M, Branson S, Branson K. JAABA: interactive machine learning for automatic annotation of animal behavior. Nat Methods. 2013;10(1):64-7.

Competing interests: The authors have no competing interests.

Data and materials availability: All data are available in the main text or the supplementary materials.

Figure Legends

Fig 1. Behavioral and anatomical screen of FBS lines.

A) Diagram of the experimental assay. Sleep was measured at 22°C (for thermogenetic activation) or with LED OFF (for the optogenetic activation protocol) for 2 days to establish baseline sleep profile. Flies were then shifted to 31°C (thermogenetic) or LEDs were turned ON (LED ON, optogenetic) for 24h at the start of day3 to increase activity of the targeted cells by activating the TrpA1 or CsChrimson channel, and then returned to 22°C or LED OFF on day4. White bars (L) represent the 12h of light and black bars (D) represent the 12h of dark that are oscillating daily.

B) Box plots of total sleep change in % ((total sleep on day3-total sleep on day2/total sleep on day2) X 100) for female control (Empty: Empty-AD; 23E10-DBD) and 20 FBS lines expressing UAS-TrpA1; UAS-mCD8GFP. The bottom and top of each box represents the first and third quartile, and the horizontal line dividing the box is the median. The whiskers represent the

10th and 90th percentiles. The gray rectangle spanning the horizontal axis indicates the interquartile range of the control. Kruskal-Wallis ANOVA followed by Dunn's multiple comparisons revealed that 4 FBS lines increase sleep significantly more than control flies when thermogenetically activated. *P<0.05, **P<0.01, ***P<0.001, ****P<0.0001, n=30-45 flies per genotype.

C) Box plots of total sleep change in % ((total sleep on day3-total sleep on day2/total sleep on day2) X 100) for vehicle-fed and retinal-fed control (Empty) and 20 FBS female flies expressing CsChrimson upon 627nm LED stimulation. The bottom and top of each box represents the first and third quartile, and the horizontal line dividing the box is the median. The whiskers represent the 10th and 90th percentiles. Two-way ANOVA followed by Sidak's multiple comparisons revealed that 6 retinal-fed FBS lines increase sleep significantly when stimulated with 627nm LEDs when compared with vehicle-fed flies. **P<0.01, ***P<0.001, ****P<0.0001, n=20-40 flies per genotype and condition.

D-H) Left, sleep profile in minutes of sleep per hour for day 2 (22°C, blue line) and day 3 (31°C, red line) for empty control (Empty-AD; 23E10-DBD, **D**), FBS42 (**E**), FBS45 (**F**), FBS53 (**G**) and FBS68 (**H**) female flies expressing TrpA1 and mCD8GFP. Right, Representative confocal stacks for each *FBS>UAS-TrpA1; UAS-mCD8GFP* line of a female brain (left panel), VNC (middle panel) as well as a magnified view of the location of VNC-SP "bowtie" processes. Green, anti-GFP; magenta, anti-nc82 (neuropile marker).

The raw data underlying parts B and C can be found in S1 Data.

Fig 2. Activation of dFB$^{23E10\cap 84C10}$ neurons promotes sleep.

A) Representative confocal stack of a female *84C10AD; 23E10-DBD (dFB-Split)>UAS-mCD8GFP* brain (left panel), VNC (middle panel), and the location where VNC-SP "bowtie" processes are seen in many FBS lines, but not in dFB-Split (right panel). We observed 22.52 ± 0.59 (n=23) dFB neurons in *dFB-Split>UAS-mCD8GFP* brains. Green, anti-GFP; magenta, anti-nc82 (neuropile marker).

B) Sleep profile in minutes of sleep per hour for day 2 (LED OFF, blue line) and day 3 (LED ON, red line) for retinal-fed empty control (Empty-AD; 23E10-DBD) and dFB-Split female flies expressing CsChrimson subjected to a 1Hz optogenetic activation protocol.

C) Box plots of total sleep change in % ((total sleep on day3-total sleep on day2/total sleep on day2) X 100) for female control (Empty-AD; 23E10-DBD) and dFB-Split flies expressing CsChrimson under 1Hz optogenetic activation (cycles of 5ms LED ON, 995ms LED OFF). Two-way ANOVA followed by Sidak's multiple comparisons revealed no differences between control and dFB-Split. n.s.= not significant. n=20-29 flies per genotype and condition.

D) Sleep profile in minutes of sleep per hour for day 2 (LED OFF, blue line) and day 3 (LED ON, red line) for retinal-fed empty control (Empty-AD; 23E10-DBD) and dFB-Split female flies expressing CsChrimson subjected to our standard optogenetic activation protocol (5ms LED ON, 95ms LED OFF, with a 4 second delay between pulses).

E) Box plots of total sleep change in % ((total sleep on day3-total sleep on day2/total sleep on day2) X 100) for female control (Empty-AD; 23E10-DBD) and dFB-Split flies expressing CsChrimson under standard optogenetic activation. Two-way ANOVA followed by Sidak's multiple comparisons revealed no differences between control and dFB-Split. n.s.= not significant. n=59-82 flies per genotype and condition.

F) Sleep profile in minutes of sleep per hour for day 2 (LED OFF, blue line) and day 3 (LED ON, red line) for retinal-fed empty control (Empty-AD; 23E10-DBD) and dFB-Split female flies expressing CsChrimson subjected to a 10Hz optogenetic activation protocol (cycles of 5ms LED ON, 95ms LED OFF).

G) Box plots of total sleep change in % for female control (Empty-AD; 23E10-DBD) and dFB-Split flies expressing CsChrimson under 10Hz optogenetic activation. Two-way ANOVA followed by Sidak's multiple comparisons revealed that sleep is significantly increased in *dFB-Split>CsChrimson* females. ***P<0.001, n.s.= not significant. n=22-24 flies per genotype and condition.

H) Sleep profile in minutes of sleep per hour for day 2 (LED OFF, blue line) and day 3 (LED ON, red line) for retinal-fed empty control (Empty-AD; 23E10-DBD) and dFB-Split female flies

expressing CsChrimson subjected to a 20Hz optogenetic activation protocol (cycles of 5ms LED ON, 45ms LED OFF).

I) Box plots of total sleep change in % for female control (Empty-AD; 23E10-DBD) and dFB-Split flies expressing CsChrimson under 20Hz optogenetic activation. Two-way ANOVA followed by Sidak's multiple comparisons revealed that sleep is significantly increased in *dFB-Split>CsChrimson* females. **P<0.01, n.s.= not significant. n=26-38 flies per genotype and condition.

J) Sleep profile in minutes of sleep per hour for day 2 (LED OFF, blue line) and day 3 (LED ON, red line) for retinal-fed empty control (Empty-AD; 23E10-DBD) and dFB-Split female flies expressing CsChrimson subjected to a 50Hz optogenetic activation protocol (cycles of 5ms LED ON, 15ms LED OFF).

K) Box plots of total sleep change in % for female control (Empty-AD; 23E10-DBD) and dFB-Split flies expressing CsChrimson under 50Hz optogenetic activation. Two-way ANOVA followed by Sidak's multiple comparisons revealed that sleep is significantly increased in *dFB-Split>CsChrimson* females. *P<0.05, ***P<0.001. n=25-38 flies per genotype and condition.

L) Box plots of total sleep change in % for female control (Empty-AD; 23E10-DBD) and dFB-Split flies expressing CsChrimson under constant optogenetic activation. Two-way ANOVA followed by Sidak's multiple comparisons revealed that sleep is significantly increased in *dFB-Split>CsChrimson* females. n.s.= not significant, ****P<0.0001. n=17-27 flies per genotype and condition.

M) Box plots of total sleep change in % for female control (Empty-AD; 23E10-DBD) and dFB-Split flies expressing CsChrimson under 20Hz optogenetic activation obtained with the DAM5H multibeam system. Two-way ANOVA followed by Sidak's multiple comparisons revealed that sleep is significantly increased in *dFB-Split>CsChrimson* females. . n.s.= not significant, **P<0.01. n=12-15 flies per genotype and condition.

N) Box plots of total sleep change in % for female control (Empty-AD; 23E10-DBD) and dFB-Split flies expressing CsChrimson under 50Hz optogenetic activation obtained with the DAM5H multibeam system. Two-way ANOVA followed by Sidak's multiple comparisons revealed that

sleep is significantly increased in *dFB-Split>CsChrimson* females. *P<0.05, **P<0.01. n=35-54 flies per genotype and condition.

O) Setup for combined multibeam and video analysis.

P) Multibeam (left) and video analysis (right) of retinal-fed control and *dFB-Split>UAS-CsChrimson* female flies. Recordings were performed between ZT3-5 for 10 minutes of baseline (Bs) followed by 10 minutes of 20Hz optogenetic activation (Act). For both multibeam and video analysis, data was analyzed in 1 minute bin. Flies could perform the following 3 behaviors, walking, micromovements (in place movements like feeding or grooming) or rest (no movements at all), and percentage of time spent in each behavior over 10 minutes is shown. If a fly walks during a minute bin, the output for that minute is walking, independently of other behaviors that could be performed during the same minute. If a fly performs a micromovement during a minute bin, but shows no walking, the output for that minute is micromovements. If a fly shows no walking or micromovements for a minute bin, the output for that minute is resting. For video analysis, behaviors were manually scored. Two-way repeated measures ANOVA followed by Sidak's multiple comparisons test found that LED activated retinal-fed *dFB-Split>UAS-CsChrimson* flies spend less time walking and more time resting than on baseline. No changes in micromovements were observed. No changes were seen in control flies. Similar results were obtained with multibeam and video analysis. n.s.= not significant, ** P<0.01, *** P<0.001. n= 11-12 flies for each genotype.

Q) Video analysis of retinal-fed control and *dFB-Split>UAS-CsChrimson* female flies. Recording was performed at ZT1-2 for 30 minutes on consecutive days during baseline (OFF) and activation (ON). Behaviors were manually scored, and amount of time spent in each behavior over 30 minutes is shown. Two-way ANOVA followed by Sidak's multiple comparisons test found that retinal-fed *dFB-Split>UAS-CsChrimson* flies with LED ON sleep significantly more than on baseline day (OFF), **** P<0.0001, but spend less time walking (**** P<0.0001), grooming (*** P<0.01), or feeding (**** P<0.0001). Rest (periods of inactivity shorter than 5 minutes) are not different. We observed no differences in time spent in all behaviors for control flies between activation and baseline days. n.s.= not significant. n= 8 flies for each genotype.

R) Arousal threshold in vehicle-fed and retinal-fed *dFB-Split>UAS-CsChrimson* female flies. Percentage of flies awakened by a stimulus of increasing strength (20%, 40%, 60%, 80% or

100% of maximum strength) with and without 627nm LEDs stimulation. Two-way ANOVA followed by Sidak's multiple comparisons indicates that activation of dFB$^{23E10\cap 84C10}$ neurons reduce the responsiveness to the 20% and 40% stimulus strength when compared with non-activated flies. No difference in responsiveness is seen at the strongest stimulus (60%, 80% and 100%). Two-way ANOVA followed by Sidak's multiple comparisons indicates that in vehicle-fed flies no difference in responsiveness is seen between LED stimulated and non-stimulated flies. ****P<0.0001, ***P<0.001, n.s.= not significant. n=16-33 flies per genotype and condition.

The raw data underlying parts C, E, G, I, K, L, M, N, P, Q and R can be found in S1 Data.

Fig 3. The sleep induced by dFB$^{23E10\cap 84C10}$ neurons activation can consolidate Long-Term Memory.

A) Schematic of protocol for LTM consolidation. A 1 h training period that only generates STM is followed by optogenetic activation of dFB$^{23E10\cap 84C10}$ neurons for 23 h post-training (with or without sleep deprivation). Flies were tested 24 h after the onset of training.

B) Post-training sleep change for different genotypes and condition. The ~23 h time period post-training was matched to the equivalent time period on the baseline day for comparison. Unpaired parametric t-test for Empty-Split groups. Kruskal-Wallis test of multiple comparisons for dFB-Split groups using the vehicle condition as the control. ****P<0.0001, **P<0.01, ns= not significant. n= 46-54 flies per genotype and condition.

C) Courtship LTM shown as the suppression index (SI, SI = 100 * (1 – (CI Trained / CI Untrained))) of trained fly groups tested 24 h after the onset of training. Wilcoxon signed-rank test using $H_{0:}$ SI = 0. Sample size (untrained:trained) from left to right on the graph, n = 54 (27:27), 51 (27:24), 49 (27:22), 51 (26:25), 46 (21:25), and 53 (27:26), respectively. Courtship indices < 10% were excluded from both groups. ***P< 0.001, ns= not significant.

The raw data underlying parts B and C can be found in S1 Data.

Fig 4. Chronic hyperpolarization of dFB$^{23E10\cap 84C10}$ neurons promotes sleep and impairs sleep homeostasis.

A) Box plots of total sleep (in minutes) for control and *dFB-Split>Kir2.1* female flies. A One-way ANOVA followed by Tukey's multiple comparisons revealed that *dFB-Split>Kir2.1* female flies sleep significantly more than controls. *P<0.05, ***P<0.001, ****P<0.0001. n=40-85 flies per genotype.

B) Box plots of locomotor activity counts per minute awake for flies presented in A. A Kruskal-Wallis ANOVA followed by Dunn's multiple comparisons revealed no differences between controls and *dFB-Split>Kir2.1* female flies. n.s.= not significant. n=40-85 flies per genotype.

C) Box plots of daytime sleep bout duration (in minutes) for flies presented in A. A Kruskal-Wallis ANOVA followed by Dunn's multiple comparisons revealed that daytime sleep bout duration is increased in *dFB-Split>Kir2.1* female flies. ****P<0.0001, **P<0.01. n=40-85 flies per genotype.

D) Box plots of nighttime sleep bout duration (in minutes) for flies presented in A. A Kruskal-Wallis ANOVA followed by Dunn's multiple comparisons revealed no differences between controls and *dFB-Split>Kir2.1* female flies. n.s.= not significant, **P<0.01. n=40-85 flies per genotype.

E) Box plots of total sleep (in minutes) for control and *dFB-Split>Kir2.1* female flies measured with the DAM5H multibeam system. A Two-tailed Mann-Whitney U test revealed that *dFB-Split>Kir2.1* female flies sleep significantly more than controls. ***P<0.001. n=49-61 flies per genotype.

F) Diagram of the experimental assay for acute silencing. Sleep was measured at 22°C for 2 days to establish baseline sleep profile. Flies were then shifted to 31°C for 24h at the start of day3 to silence the activity of the targeted cells by activating the Shi^{ts1} actuator, and then returned to 22°C on day4. White bars (L) represent the 12h of light and black bars (D) represent the 12h of dark that are oscillating daily.

G) Box plots of total sleep change in % for control (*Empty-AD; 23E10-DBD>UAS-Shi^{ts1}*), and *dFB-Split>UAS-Shi^{ts1}* female flies upon thermogenetic silencing. A Two-tailed unpaired t test revealed no differences between controls and *dFB-Split>UAS-Shi^{ts1}* female flies. n.s.= not significant. n=50 flies per genotype.

H) Box plots of total sleep change in % for control (*Empty-AD; 23E10-DBD>UAS-Shi*^{ts1}), and *dFB-Split>UAS-Shi*^{ts1} male flies upon thermogenetic silencing. A Two-tailed unpaired t test revealed no differences between controls and *dFB-Split>UAS-Shi*^{ts1} male flies. n.s.= not significant. n=60-62 flies per genotype.

I) Cumulative sleep lost then gained for *Empty-AD; 23E10-DBD>UAS-Kir2.1* and *dFB-Split>UAS-Kir2.1* female flies during 12h of mechanical sleep deprivation (D+SD) and 48h of sleep recovery.

J) Box plots of total sleep recovered in % during 48h of sleep recovery following 12h of sleep deprivation at night for *Empty-AD; 23E10-DBD>UAS-Kir2.1* and *dFB-Split>UAS-Kir2.1* female flies. Two-tailed Mann-Whitney U tests revealed that sleep rebound is significantly decreased at all time points between controls and *dFB-Split>UAS-Kir2.1* female flies. However, Wilcoxon signed-rank tests (indicated by $^{\#}$ on graph) using $H_{0:}$ % sleep recovered = 0 revealed that *dFB-Split>UAS-Kir2.1* female flies have a sleep rebound significantly greater than 0 at time points 4h, 6h, 12h, and 24h. ***P<0.001, ****P<0.0001, $^{\#\#\#\#}$P<0.0001, $^{\#\#\#}$P<0.001, $^{\#}$P<0.5, n.s.= not significant. n=25-54 flies per genotype.

The raw data underlying parts A, B, C, D, E, G, H, I, and J can be found in S1 Data.

Fig 5. Neurochemical identity of dFB$^{23E10\cap 84C10}$ neurons.

A) Representative confocal stack of a female *dFB-Split>UAS-mCD8GFP* brain stained with GFP and GABA antibodies and focusing on dFB$^{23E10\cap 84C10}$ cell bodies. Green, anti-GFP; magenta, anti-GABA.

B) Representative confocal stack of a female *dFB-Split>UAS-mCD8GFP* brain stained with GFP, VGlut and ChAT antibodies and focusing on dFB$^{23E10\cap 84C10}$ cell bodies. White arrow indicates a VGlut only positive dFB$^{23E10\cap 84C10}$ neurons. Yellow arrows show ChAT only positive dFB$^{23E10\cap 84C10}$ neurons. Yellow asterisks indicate dFB$^{23E10\cap 84C10}$ neurons positive for VGlut and ChAT. Green, anti-GFP; gray, anti-VGlut, magenta, anti-ChAT.

C) Quantification of VGlut only positive, ChAT only positive and VGlut and ChAT positive dFB$^{23E10\cap 84C10}$ neurons. We observed 22.76± 0.58 (n=13) GFP positive dFB$^{23E10\cap 84C10}$ neurons

per brain, 3.31± 0.71 cells were ChAT only positive, 4.69± 0.73 cells were VGlut only positive, 13.77± 0.93 cells were ChAT and VGlut positive, and 0.85± 0.25 cells were negative for both ChAT and VGlut.

D) Representative confocal stack of a female *84C10-AD; Gad1-DBD>UAS-mCD8GFP*. Green, anti-GFP; magenta, anti-nc82 (neuropile marker).

E) Representative confocal stack of a female *84C10-AD; ChAT-DBD>UAS-mCD8GFP*. Green, anti-GFP; magenta, anti-nc82 (neuropile marker).

F) Representative confocal stack of a female *VGlut-AD; 84C10-DBD>UAS-mCD8GFP*. Green, anti-GFP; magenta, anti-nc82 (neuropile marker).

G) Quantification of the numbers of dFB neurons contained within the 2 Split-GAL4 lines presented in E and F. We observed 16.00± 0.41 (n=4) dFB cells for *84C10-AD; ChAT-DBD* and 22.20± 0.49 (n=5) dFB neurons for *VGlut-AD; 84C10-DBD.* No other expression was seen in the brain and VNC for these lines.

H) Sleep profile in minutes of sleep per hour for day 2 (LED OFF, blue line) and day 3 (LED ON, red line) for retinal-fed Empty-Split control females expressing CsChrimson subjected to a 50Hz optogenetic activation protocol (cycles of 5ms LED ON, 15ms LED OFF).

I) Sleep profile in minutes of sleep per hour for day 2 (LED OFF, blue line) and day 3 (LED ON, red line) for retinal-fed *VGlut-AD; 84C10-DBD>CsChrimson* female flies subjected to a 50Hz optogenetic activation protocol (cycles of 5ms LED ON, 15ms LED OFF).

J) Sleep profile in minutes of sleep per hour for day 2 (LED OFF, blue line) and day 3 (LED ON, red line) for retinal-fed *84C10-AD; ChAT-DBD>CsChrimson* female flies subjected to a 50Hz optogenetic activation protocol (cycles of 5ms LED ON, 15ms LED OFF).

K) Box plots of total sleep change in % ((total sleep on activation day-total sleep on baseline day/total sleep on baseline day) X 100) for control (*Empty-Split>CsChrimson*), *VGlut-AD; 84C10-DBD>CsChrimson* and *84C10-AD; ChAT-DBD>CsChrimson* female flies under a 50Hz optogenetic activation protocol. Two-way ANOVA followed by Sidak's multiple comparisons revealed that activating 84C10-AD; ChAT-DBD neurons significantly increases sleep. n.s.= not significant, ****P<0.0001. n=32-47 flies per genotype and condition.

L) Box plots of daytime sleep change in % ((daytime sleep on activation day-daytime sleep on baseline day/daytime sleep on baseline day) X 100) for control (*Empty-Split>CsChrimson*), *VGlut-AD; 84C10-DBD>CsChrimson* and *84C10-AD; ChAT-DBD>CsChrimson* female flies under a 50Hz optogenetic activation protocol. Two-way ANOVA followed by Tukey's multiple comparisons revealed that activating 84C10-AD; ChAT-DBD and VGlut-AD; 84C10-DBD neurons significantly increases daytime sleep and that activating 84C10-AD; ChAT-DBD neurons increase sleep more than activation of VGlut-AD; 84C10-DBD cells. n.s.= not significant, ***P<0.001, ****P<0.0001. n=32-47 flies per genotype and condition.

M) Sleep profile in minutes of sleep per hour for *Empty-Split>Shi^{ts1}* females maintained at 22° (baseline) and 31° (activation).

N) Sleep profile in minutes of sleep per hour for *VGlut-AD; 84C10-DBD>Shi^{ts1}* females maintained at 22° (baseline) and 31° (activation).

O) Sleep profile in minutes of sleep per hour for *84C10-AD; ChAT-DBD>Shi^{ts1}* females maintained at 22° (baseline) and 31° (activation).

P) Box plots of total sleep change in % ((total sleep on activation day-total sleep on baseline day/total sleep on baseline day) X 100) for control (*Empty-Split>Shi^{ts1}*), *VGlut-AD; 84C10-DBD>Shi^{ts1}* and *84C10-AD; ChAT-DBD>Shi^{ts1}* female flies. A Kruskal-Wallis ANOVA followed by Dunn's multiple comparisons revealed that acutely silencing VGlut-AD; 84C10-DBD and 84C10-AD; ChAT-DBD neurons significantly decreases sleep. ****P<0.0001. n=26-60 flies per genotype.

Q) Box plots of locomotor activity counts per minute awake for flies presented in P. Two-way repeated measures ANOVA followed by Sidak's multiple comparisons revealed that acutely silencing VGlut-AD; 84C10-DBD and 84C10-AD; ChAT-DBD neurons does not lead to hyperactivity. n.s.= not significant, *P<0.05, ****P<0.0001. n=26-60 flies per genotype.

R) Box plots of total sleep recovered in % during 24h of recovery following 12h of sleep deprivation at night for *Empty-Split>Shi^{ts1}*, *VGlut-AD; 84C10-DBD>Shi^{ts1}* and *84C10-AD; ChAT-DBD>Shi^{ts1}* female flies. Following sleep deprivation, flies were either maintained at 22° (control) or at 31° (to silence neurons). Kruskal-Wallis test followed by Dunn's multiple comparisons revealed that acutely silencing 84C10-AD; ChAT-DBD neurons blocks sleep

homeostasis. No differences were seen between lines at 22°. n.s.= not significant, **P<0.01, ****P<0.0001. n=28-57 flies per genotype and condition.

The raw data underlying parts C, G, K, L, P, Q, and R can be found in S1 Data.

Supporting Information

S1 Fig. Additional sleep profiles and confocal images of FBS lines.

A-P) Sleep profile (left) and representative confocal stacks (right) for brain and VNC of female *FBS>UAS-TrpA1; UAS-mCD8GFP* for 16 FBS lines not presented in Fig 1.

S2 Fig. Additional sleep parameters for FBS female flies thermogenetically activated.

A) Box plots of locomotor activity counts per minute awake for flies presented in Fig 1B. The bottom and top of each box represents the first and third quartile, and the horizontal line dividing the box is the median. The whiskers represent the 10th and 90th percentiles. Two-way repeated measures ANOVA followed by Sidak's multiple comparisons test found that for 2 sleep-promoting FBS lines (FBS45 and FBS53) locomotor activity per awake time is increased while no differences are seen for the other 2 sleep-promoting lines between 22°C and 31°C. **P<0.01, ****P<0.0001, n=30-45 flies per genotype.

B) Box plots of daytime sleep bout duration in minutes for flies presented in Fig 1B. Two-way repeated measures ANOVA followed by Sidak's multiple comparisons test revealed that 7 FBS lines show a significant increase in daytime sleep bout duration between 22°C and 31°C. *P<0.05, **P<0.01, ***P<0.001, ****P<0.0001, n=30-45 flies per genotype.

C) Box plots of nighttime sleep bout duration in minutes for flies presented in Fig 1B. Two-way repeated measures ANOVA followed by Sidak's multiple comparisons test revealed that control

and most FBS lines show a significant decrease in nighttime sleep bout duration between 22°C and 31°C. Only 4 sleep-promoting FBS lines show no difference between 22°C and 31°C. Dunnett's multiple comparisons reveal that for 3 of them, nighttime sleep bout duration at 31°C is significantly increased compared with Empty control flies (# on figure). **P<0.01, ***P<0.001, ****P<0.0001, n.s.= not significant. n=30-45 flies per genotype.

The raw data underlying parts A, B, and C can be found in S1 Data.

S3 Fig. Thermogenetic activation in male flies.

A) Box plots of total sleep change in % ((total sleep on day3-total sleep on day2/total sleep on day2) X 100) for male control (Empty-AD; 23E10-DBD) and 20 FBS lines expressing UAS-TrpA1; UAS-mCD8GFP. The gray rectangle spanning the horizontal axis indicates the interquartile range of the control. Kruskal-Wallis ANOVA followed by Dunn's multiple comparisons revealed that 7 FBS lines increase sleep significantly more than control flies when transferred to 31°C. *P<0.05, ****P<0.0001, n=26-47 flies per genotype.

B) Box plots of locomotor activity counts per minute awake for flies presented in A. Two-way repeated measures ANOVA followed by Sidak's multiple comparisons test found that for 3 sleep-promoting FBS lines (FBS45, FBS53 and FBS68) locomotor activity per awake time is increased while no differences are seen for the other 4 sleep-promoting lines between 22°C and 31°C. *P<0.05, **P<0.01, ***P<0.001, ****P<0.0001, n=26-47 flies per genotype.

C) Box plots of daytime sleep bout duration for flies presented in A. Two-way repeated measures ANOVA followed by Sidak's multiple comparisons test found that for 6 out of the 7 sleep-promoting FBS lines, daytime sleep bout duration is significantly increased at 31°C compared with 22°C. **P<0.01, ***P<0.001, ****P<0.0001, n=26-47 flies per genotype.

D) Box plots of nighttime sleep bout duration for flies presented in A. Two-way repeated measures ANOVA followed by Sidak's multiple comparisons revealed that control and most FBS lines show a significant decrease in nighttime sleep bout duration between 22°C and 31°C. 4 sleep-promoting FBS lines show no difference between 22°C and 31°C (FBS42, FBS53, FBS81 and FBS84) while FBS45 and FBS68 show an increase in nighttime sleep bout duration at 31°C. **P<0.01, ****P<0.0001, n=26-47 flies per genotype.

The raw data underlying parts A, B, C, and D can be found in S1 Data.

S4 Fig. Additional sleep profiles for FBS lines in optogenetic screen.

Sleep profiles in minutes of sleep per hour for vehicle-fed and retinal-fed FBS lines in optogenetic screen.

S5 Fig. Optogenetic activation in males.

A) Box plots of total sleep change in % ((total sleep on day3-total sleep on day2/total sleep on day2) X 100) for control (Empty) and 20 experimental vehicle-fed and retinal-fed male flies expressing CsChrimson upon 627nm LED stimulation. Two-way ANOVA followed by Sidak's multiple comparisons revealed that 8 retinal-fed FBS lines increase sleep significantly when stimulated with 627nm LEDs when compared with vehicle-fed flies. *P<0.05, **P<0.01, ****P<0.0001. n=20-44 flies per genotype and condition.

B) Box plots of locomotor activity counts per minute awake for retinal-fed flies presented in A. Two-way repeated measures ANOVA followed by Sidak's multiple comparisons test found that for most sleep-promoting FBS lines, locomotor activity per awake time is not affected when the flies are stimulated with 627nm LEDs while it is increased in *FBS72>UAS-CsChrimson* flies. *P<0.05, n=24-44 flies per genotype.

C) Box plots of daytime sleep bout duration (in minutes) for retinal-fed flies presented in A. Two-way repeated measures ANOVA followed by Sidak's multiple comparisons indicate that daytime sleep bout duration is increased in 11 FBS lines expressing CsChrimson when stimulated with 627nm LEDs. *P<0.05, ***P<0.001, ****P<0.0001, n=24-44 flies per genotype.

D) Box plots of nighttime sleep bout duration (in minutes) for retinal-fed flies presented in A. Two-way repeated measures ANOVA followed by Sidak's multiple comparisons indicate that nighttime sleep bout duration is increased in 6 FBS lines expressing CsChrimson when stimulated with 627nm LEDs. **P<0.01, ****P<0.0001, n=24-44 flies per genotype.

The raw data underlying parts A, B, C, and D can be found in S1 Data.

S6 Fig. Additional data for retinal-fed females in optogenetic activation.

A) Box plots of locomotor activity counts per minute awake for retinal-fed flies presented in Fig 1C. The bottom and top of each box represents the first and third quartile, and the horizontal line dividing the box is the median. The whiskers represent the 10th and 90th percentiles. Two-way repeated measures ANOVA followed by Sidak's multiple comparisons test found that for most sleep-promoting FBS lines, locomotor activity per awake time is not affected when the flies are stimulated with 627nm LEDs while it is increased in *FBS45>UAS-CsChrimson* flies. ****P<0.0001, n=21-40 flies per genotype.

B) Box plots of daytime sleep bout duration (in minutes) for retinal-fed flies presented in Fig 1C. The bottom and top of each box represents the first and third quartile, and the horizontal line dividing the box is the median. The whiskers represent the 10th and 90th percentiles. Two-way repeated measures ANOVA followed by Sidak's multiple comparisons indicate that daytime sleep bout duration is increased in 9 FBS lines expressing CsChrimson when stimulated with 627nm LEDs. *P<0.05, **P<0.01, ***P<0.001, ****P<0.0001, n=21-40 flies per genotype.

C) Box plots of nighttime sleep bout duration (in minutes) for retinal-fed flies presented in Fig 1C. The bottom and top of each box represents the first and third quartile, and the horizontal line dividing the box is the median. The whiskers represent the 10th and 90th percentiles. Two-way repeated measures ANOVA followed by Sidak's multiple comparisons indicate that nighttime sleep bout duration is increased in 6 FBS lines expressing CsChrimson when stimulated with 627nm LEDs. *P<0.05, ****P<0.0001, n=21-40 flies per genotype.

The raw data underlying parts A, B, and C can be found in S1 Data.

S7 Fig. Vehicle-fed sleep data for females in optogenetic experiments.

A) Box plots of locomotor activity counts per minute awake for vehicle-fed flies presented in Fig 1C. Two-way repeated measures ANOVA followed by Sidak's multiple comparisons test found that all lines except FBS42 show no difference in locomotor activity per awake time when the flies are stimulated with 627nm LEDs. ***P<0.001. n=20-39 flies per genotype.

B) Box plots of daytime sleep bout duration for vehicle-fed flies presented in Fig 1C. Two-way repeated measures ANOVA followed by Sidak's multiple comparisons test found that most vehicle-fed sleep-promoting lines show no difference in daytime sleep bout duration when the flies are stimulated with 627nm LEDs. *P<0.05, **P<0.01, ***P<0.001. n=20-39 flies per genotype.

C) Box plots of nighttime sleep bout duration for vehicle-fed flies presented in Fig 1C. Two-way repeated measures ANOVA followed by Sidak's multiple comparisons test show no difference in nighttime sleep bout duration when vehicle-fed flies are stimulated with 627nm LEDs. n=20-39 flies per genotype.

The raw data underlying parts A, B, and C can be found in S1 Data.

S8 Fig. Vehicle-fed sleep data for males in optogenetic experiments.

A) Box plots of locomotor activity counts per minute awake for vehicle-fed flies presented in S5A Fig. Two-way repeated measures ANOVA followed by Sidak's multiple comparisons test found no difference in locomotor activity per awake time when the flies are stimulated with 627nm LEDs. n=20-40 flies per genotype.

B) Box plots of daytime sleep bout duration for vehicle-fed flies presented in S5A Fig. Two-way repeated measures ANOVA followed by Sidak's multiple comparisons test found that most vehicle-fed sleep-promoting lines show no difference in daytime sleep bout duration when the flies are stimulated with 627nm LEDs. *P<0.05, **P<0.01, ****P<0.0001. n=20-40 flies per genotype.

C) Box plots of nighttime sleep bout duration for vehicle-fed flies presented in S5A Fig. Two-way repeated measures ANOVA followed by Sidak's multiple comparisons test show no difference in nighttime sleep bout duration when vehicle-fed flies are stimulated with 627nm LEDs. n=20-40 flies per genotype.

The raw data underlying parts A, B, and C can be found in S1 Data.

S9 Fig. VNC-SP neurons are present in sleep-promoting FBS lines.

A) Representative confocal stacks of *FBS42>UAS-GFP* (left) and *FBS42>UAS-GFP; ChAT-LexA>2x LexAop2KZip*$^{+}$ (right) female flies showing the location of the VNC-SP bowtie processes, the dFB region, the VNC and VNC-SP neurons. Expression of GFP in VNC-SP neurons and in their bowtie brain processes is abolished by the expression of the KZip^{+} repressor. Gray arrows show VNC-SP neurons. Green, anti-GFP; magenta, anti-nc82.

B) Representative confocal stacks of *FBS45>UAS-GFP* (left) and *FBS45>UAS-GFP; ChAT-LexA> LexAop2KZip*$^{+}$ (right) female flies showing the location of the VNC-SP bowtie processes, the dFB region, the VNC and VNC-SP neurons. Expression of GFP in VNC-SP neurons and in their bowtie brain processes is abolished by the expression of the KZip^{+} repressor. Gray arrows show VNC-SP neurons. Green, anti-GFP; magenta, anti-nc82.

C) Representative confocal stacks of *FBS53>UAS-GFP* (left) and *FBS53>UAS-GFP; ChAT-LexA> LexAop2KZip*$^{+}$ (right) female flies showing the location of the VNC-SP bowtie processes, the dFB region, the VNC and VNC-SP neurons. Expression of GFP in VNC-SP neurons and in their bowtie brain processes is abolished by the expression of the KZip^{+} repressor. Gray arrows show VNC-SP neurons. Green, anti-GFP; magenta, anti-nc82.

D) Representative confocal stacks of *FBS68>UAS-GFP* (left) and *FBS68>UAS-GFP; ChAT-LexA> 2x LexAop2KZip*$^{+}$ (right) female flies showing the location of the VNC-SP bowtie processes, the dFB region, the VNC and VNC-SP neurons. Expression of GFP in VNC-SP neurons and in their bowtie brain processes is abolished by the expression of the KZip^{+} repressor. Gray arrows show VNC-SP neurons. Green, anti-GFP; magenta, anti-nc82.

E) Box plots of total sleep change in % ((total sleep on day3-total sleep on day2/total sleep on day2) X 100) for female control (Empty: Empty-AD; 23E10-DBD) and 4 sleep-promoting FBS lines expressing UAS-TrpA1 or UAS-TrpA1 and the KZip^{+} repressor in cholinergic neurons (ChAT-KZip^{+}). Two-way ANOVA followed by Sidak's multiple comparisons revealed that repressing the expression of TrpA1 in cholinergic neurons abolishes the sleep increases obtained when thermogenetically activating all 4 FBS lines. ****P<0.0001, n.s.= not significant. $^{\#}$ indicates that sleep is significantly increased compared with *Empty>TrpA1* controls. n=17-69 flies per genotype.

The raw data underlying part E can be found in S1 Data.

S10 Fig. Differential strength of expression in VNC-SP neurons for different FBS lines.

A) Schematic of the GFP.DD experimental design.

B) Representative confocal stacks of females 23E10-GAL4, VNC-SP Split, FBS1, FBS33, FBS45, and FBS58 expressing GFP-DD and fed DMSO or TMP for 24h before dissection. Stacks are focused on the metathoracic region of the VNC where VNC-SP cell bodies are located. Green, anti-GFP. White asterisks indicate VNC-SP cell bodies.

C) Quantification of staining intensity for data presented in B. Two-way ANOVA followed by Sidak's multiple comparisons revealed that there is significantly more GFP staining in VNC-SP neurons in 23E10-GAL4, VNC-SP Split, FBS33, and FBS45 fed TMP compared with DMSO fed flies. n.s= not significant, **P<0.01, ****P<0.0001. n=5-14 VNC per genotype and condition.

The raw data underlying part C can be found in S1 Data.

S11 Fig. Expression pattern of dFB-Split.

Representative confocal stack images of adult tissues from *Empty-AD; 23E10-DBD > UAS-mCD8GFP* (top) and *dFB-Split> UAS-mCD8GFP* (bottom) female flies. GFP is expressed in the brain, but not the wings, legs, ovaries, or gut in dFB-Split. Tissue was dissected, fixed, and stained with DAPI. Green, anti-GFP; Blue, DAPI.

S12 Fig. Additional data for optogenetic activation of dFB$^{23E10\cap 84C10}$ neurons at 10Hz.

A) Box plots of locomotor activity counts per minute awake for retinal-fed flies presented in Fig 2G. The bottom and top of each box represents the first and third quartile, and the horizontal line dividing the box is the median. The whiskers represent the 10th and 90th percentiles. Two-way repeated measures ANOVA followed by Sidak's multiple comparisons test found no difference in locomotor activity per awake time when the flies are stimulated at 10Hz with 627nm LEDs. n.s= not significant. n=23-24 flies per genotype.

B) Box plots of daytime sleep bout duration (in minutes) for retinal-fed flies presented in Fig 2G. The bottom and top of each box represents the first and third quartile, and the horizontal line dividing the box is the median. The whiskers represent the 10th and 90th percentiles. Two-way repeated measures ANOVA followed by Sidak's multiple comparisons indicate that daytime sleep bout duration is increased in *dFB-Split>CsChrimson* female flies when stimulated with 627nm LEDs at 10Hz. n.s= not significant, ***P<0.001. n=23-24 flies per genotype.

C) Box plots of nighttime sleep bout duration (in minutes) for retinal-fed flies presented in Fig 2G. The bottom and top of each box represents the first and third quartile, and the horizontal line dividing the box is the median. The whiskers represent the 10th and 90th percentiles. Two-way repeated measures ANOVA followed by Sidak's multiple comparisons found no differences in nighttime sleep bout duration. n.s= not significant. n=23-24 flies per genotype.

D) Box plots of locomotor activity counts per minute awake for vehicle-fed flies presented in Fig 2G. The bottom and top of each box represents the first and third quartile, and the horizontal line dividing the box is the median. The whiskers represent the 10th and 90th percentiles. Two-way repeated measures ANOVA followed by Sidak's multiple comparisons test found no difference in locomotor activity per awake time when the flies are stimulated at 10Hz with 627nm LEDs. n.s= not significant. n=22 flies per genotype.

E) Box plots of daytime sleep bout duration (in minutes) for vehicle-fed flies presented in Fig 2G. The bottom and top of each box represents the first and third quartile, and the horizontal line dividing the box is the median. The whiskers represent the 10th and 90th percentiles. Two-way repeated measures ANOVA followed by Sidak's multiple comparisons found no differences in daytime sleep bout duration. n.s= not significant. n=22 flies per genotype.

F) Box plots of nighttime sleep bout duration (in minutes) for vehicle-fed flies presented in Fig 2G. The bottom and top of each box represents the first and third quartile, and the horizontal line dividing the box is the median. The whiskers represent the 10th and 90th percentiles. Two-way repeated measures ANOVA followed by Sidak's multiple comparisons. ****P<0.0001. n=22 flies per genotype.

The raw data underlying parts A, B, C, D, E, and F can be found in S1 Data.

S13 Fig. Additional data for optogenetic activation of dFB$^{23E10\cap 84C10}$ neurons at 20Hz.

A) Box plots of locomotor activity counts per minute awake for retinal-fed flies presented in Fig 2I. Two-way repeated measures ANOVA followed by Sidak's multiple comparisons test found no difference in locomotor activity per awake time when the flies are stimulated with 627nm LEDs. n.s.= not significant. n=34-38 flies per genotype.

B) Box plots of daytime sleep bout duration for retinal-fed flies presented in Fig 2I. Two-way repeated measures ANOVA followed by Sidak's multiple comparisons test found that daytime sleep bout duration is significantly increased in *dFB-Split>CsChrimson* female flies that are stimulated with 627nm LEDs. ****P<0.0001, n.s.= not significant. n=34-38 flies per genotype.

C) Box plots of nighttime sleep bout duration for retinal-fed flies presented in Fig 2I. Two-way repeated measures ANOVA followed by Sidak's multiple comparisons test found that nighttime sleep bout duration is significantly increased in *dFB-Split>CsChrimson* female flies that are stimulated with 627nm LEDs. *P<0.05, n.s.= not significant. n=34-38 flies per genotype.

D) Box plots of locomotor activity counts per minute awake for vehicle-fed flies presented in Fig 2I. Two-way repeated measures ANOVA followed by Sidak's multiple comparisons test found no difference in locomotor activity per awake time when the flies are stimulated with 627nm LEDs. n.s.= not significant. n=26-32 flies per genotype.

E) Box plots of daytime sleep bout duration for vehicle-fed flies presented in Fig 2I. Two-way repeated measures ANOVA followed by Sidak's multiple comparisons test found no difference in daytime sleep bout duration when the flies are stimulated with 627nm LEDs. n.s.= not significant. n=26-32 flies per genotype.

F) Box plots of nighttime sleep bout duration for vehicle-fed flies presented in Fig 2I. Two-way repeated measures ANOVA followed by Sidak's multiple comparisons test. ****P<0.0001. n=26-32 flies per genotype.

G) Box plots of total sleep change in % for male control (Empty-AD; 23E10-DBD) and dFB-Split flies expressing CsChrimson under 20Hz optogenetic activation. Two-way ANOVA followed by Sidak's multiple comparisons revealed that sleep is significantly increased in *dFB-*

Split>CsChrimson males. n.s.= not significant, *P<0.05. n=31-41 flies per genotype and condition.

H) Box plots of locomotor activity counts per minute awake for retinal-fed flies presented in G. Two-way repeated measures ANOVA followed by Sidak's multiple comparisons test found no difference in locomotor activity per awake time when the flies are stimulated with 627nm LEDs. n.s.= not significant. n=35-41 flies per genotype.

I) Box plots of daytime sleep bout duration for retinal-fed flies presented in G. Two-way repeated measures ANOVA followed by Sidak's multiple comparisons test found that daytime sleep bout duration is significantly increased in *dFB-Split>CsChrimson* male flies that are stimulated with 627nm LEDs. ****P<0.0001, n.s.= not significant. n=35-41 flies per genotype.

J) Box plots of nighttime sleep bout duration for retinal-fed flies presented in G. Two-way repeated measures ANOVA followed by Sidak's multiple comparisons test found that nighttime sleep bout duration is significantly increased in *dFB-Split>CsChrimson* male flies that are stimulated with 627nm LEDs. ****P<0.0001, n.s.= not significant. n=35-41 flies per genotype.

K) Box plots of locomotor activity counts per minute awake for vehicle-fed flies presented in G. Two-way repeated measures ANOVA followed by Sidak's multiple comparisons test. ***P<0.001, ****P<0.0001. n=31-36 flies per genotype.

L) Box plots of daytime sleep bout duration for vehicle-fed flies presented in G. Two-way repeated measures ANOVA followed by Sidak's multiple comparisons test found no difference in vehicle-fed males. n.s.= not significant. n=31-36 flies per genotype.

M) Box plots of nighttime sleep bout duration for vehicle-fed flies presented in G. Two-way repeated measures ANOVA followed by Sidak's multiple comparisons test show no difference in nighttime sleep bout duration when vehicle-fed flies are stimulated with 627nm LEDs. n.s.= not significant. n=31-36 flies per genotype.

The raw data underlying parts A, B, C, D, E, F, G, H, I, J, K, L, and M can be found in S1 Data.

S14 Fig. Additional data for optogenetic activation of dFB$^{23E10\cap 84C10}$ neurons at 50Hz.

A) Box plots of locomotor activity counts per minute awake for retinal-fed flies presented in Fig 2K. Two-way repeated measures ANOVA followed by Sidak's multiple comparisons test found no difference in locomotor activity per awake time in *dFB-Split>CsChrimson* female flies that are stimulated with 627nm LEDs. **P<0.01, n.s.= not significant. n=33-38 flies per genotype.

B) Box plots of daytime sleep bout duration for retinal-fed flies presented in Fig 2K. Two-way repeated measures ANOVA followed by Sidak's multiple comparisons test found that daytime sleep bout duration is significantly increased in *dFB-Split>CsChrimson* female flies that are stimulated with 627nm LEDs. ****P<0.0001, n.s.= not significant. n=33-38 flies per genotype.

C) Box plots of nighttime sleep bout duration for retinal-fed flies presented in Fig 2K. Two-way repeated measures ANOVA followed by Sidak's multiple comparisons test found that nighttime sleep bout duration is significantly increased in *dFB-Split>CsChrimson* female flies that are stimulated with 627nm LEDs. ****P<0.0001, n.s.= not significant. n=33-38 flies per genotype.

D) Box plots of locomotor activity counts per minute awake for vehicle-fed flies presented in Fig 2K. Two-way repeated measures ANOVA followed by Sidak's multiple comparisons test. *P<0.05, n.s.= not significant. n=25-31 flies per genotype.

E) Box plots of daytime sleep bout duration for vehicle-fed flies presented in Fig 2K. Two-way repeated measures ANOVA followed by Sidak's multiple comparisons test found no difference in daytime sleep bout duration when the flies are stimulated with 627nm LEDs. n.s.= not significant. n=25-31 flies per genotype.

F) Box plots of nighttime sleep bout duration for vehicle-fed flies presented in Fig 2K. Two-way repeated measures ANOVA followed by Sidak's multiple comparisons test. **P<0.01, n.s.= not significant. n=25-31 flies per genotype.

G) Box plots of total sleep change in % for male control (Empty-AD; 23E10-DBD) and dFB-Split flies expressing CsChrimson under 50Hz optogenetic activation. Two-way ANOVA followed by Sidak's multiple comparisons revealed that sleep is significantly increased in *dFB-Split>CsChrimson* males. n.s.= not significant, ***P<0.001. n=62-73 flies per genotype and condition.

H) Box plots of locomotor activity counts per minute awake for retinal-fed flies presented in G. Two-way repeated measures ANOVA followed by Sidak's multiple comparisons test. ****P<0.0001, n.s.= not significant. n=62-71 flies per genotype.

I) Box plots of daytime sleep bout duration for retinal-fed flies presented in G. Two-way repeated measures ANOVA followed by Sidak's multiple comparisons test found that daytime sleep bout duration is significantly increased in *dFB-Split>CsChrimson* female flies that are stimulated with 627nm LEDs. ****P<0.0001, n.s.= not significant. n=62-71 flies per genotype.

J) Box plots of nighttime sleep bout duration for retinal-fed flies presented in G. Two-way repeated measures ANOVA followed by Sidak's multiple comparisons test show no difference in nighttime sleep bout duration when retinal-fed flies are stimulated with 627nm LEDs. n.s.= not significant. n=62-71 flies per genotype.

K) Box plots of locomotor activity counts per minute awake for vehicle-fed flies presented in G. Two-way repeated measures ANOVA followed by Sidak's multiple comparisons test. **P<0.01, n.s.= not significant. n=63-73 flies per genotype.

L) Box plots of daytime sleep bout duration for vehicle-fed flies presented in G. Two-way repeated measures ANOVA followed by Sidak's multiple comparisons test found no difference in daytime sleep bout duration when the flies are stimulated with 627nm LEDs. n.s.= not significant. n=63-73 flies per genotype.

M) Box plots of nighttime sleep bout duration for vehicle-fed flies presented in G. Two-way repeated measures ANOVA followed by Sidak's multiple comparisons test. **P<0.01. n=63-73 flies per genotype.

The raw data underlying parts A, B, C, D, E, F, G, H, I, J, K, L, and M can be found in S1 Data.

S15 Fig. Validation of the multibeam system.

A) Setup for combined multibeam and video analysis.
B) Observed % time spent in each of 7 behaviors (Rest, Walking, Feeding, Grooming, Posture change, Proboscis extension, and single leg movement) for 19 Cs flies during 10 minutes recording.

C) Sensitivity (ratio of minutes with a behavior identified by the multibeam system to all visually labeled minutes of the same behavior) and accuracy (ratio of correctly identified minutes with a behavior by the multibeam system to all identified minutes with the same behavior by the multibeam system) of the multibeam system for identifying all behaviors. For the accuracy calculation, all micromovements (Feeding, Grooming, Posture change, Proboscis extension, and single leg movement) were pooled together.

D) Comparison of multibeam analysis and video observation for 4 Cs flies during 10 minutes.

E) Comparison of multibeam analysis and video observation for the 4 Cs flies shown in S3 Movie.

The raw data underlying parts B, C, and E can be found in S1 Data.

S16 Fig. Courtship indices for untrained and trained flies.

A) Courtship index values for male flies in untrained and trained groups for each condition presented in Fig 3C. Unpaired parametric t-test for each group of untrained and trained males for each condition. Sample size (untrained:trained) from left to right on the graph, n = 54 (27:27), 51 (27:24), 49 (27:22), 51 (26:25), 46 (21:25), and 53 (27:26), respectively. Courtship indices < 10% were excluded from both groups. **P< 0.01, ns= not significant.

The raw data underlying part A can be found in S1 Data.

S17 Fig. Additional data for hyperpolarization of dFB$^{23E10\cap 84C10}$ neurons.

A) Representative brain confocal stack of *dFB-Split>UAS-mCD8GFP*. Green, anti-GFP; magenta, anti-nc82.

B) Representative brain confocal stack of *dFB-Split>UAS-Kir2.1.EGFP*. We observed 23.40 ± 0.75 (n=5) dFB$^{23E10\cap 84C10}$ neurons in *dFB-Split>UAS-Kir2.1.EGFP* brains. This number is similar to what we have observed for *dFB-Split>UAS-mCD8GFP* brains (Fig 2A). Green, anti-GFP; magenta, anti-nc82.

C) Box plots of total sleep (in minutes) for control and *dFB-Split>Kir2.1* male flies. A Two-tailed Mann-Whitney U test revealed that *dFB-Split>Kir2.1* male flies sleep significantly more than controls. ****P<0.0001. n=69-75 flies per genotype.

D) Box plots of locomotor activity counts per minute awake for flies presented in C. A Two-tailed Mann-Whitney U test revealed no differences between controls and *dFB-Split>Kir2.1* male flies. n.s.= not significant. n=69-75 flies per genotype.

E) Box plots of daytime sleep bout duration (in minutes) for flies presented in C. A Two-tailed Mann-Whitney U test revealed that daytime sleep bout duration is increased in *dFB-Split>Kir2.1* male flies. **P<0.01. n=69-75 flies per genotype.

F) Box plots of nighttime sleep bout duration (in minutes) for flies presented in C. A Two-tailed Mann-Whitney U test revealed that nighttime sleep bout duration is increased in *dFB-Split>Kir2.1* male flies. ***P<0.001. n=69-75 flies per genotype.

The raw data underlying parts B, C, D, E, and F can be found in S1 Data.

S18 Fig. The dFB is not GABAergic.

A) Representative confocal stack of a female *23E10-GAL4>UAS-mCD8GFP* brain stained with GFP and GABA antibodies and focusing on dFB cell bodies. Green, anti-GFP; magenta, anti-GABA.

B) Representative confocal stack of a female *Gad1-AD; 23E10-DBD>UAS-mCD8GFP* brain and VNC. Green, anti-GFP; magenta, anti-nc82 (neuropile marker).

C) Representative confocal stack of a female *VGlut-AD (84713); 23E10-DBD>UAS-mCD8GFP* brain. Yellow and red arrows show non-dFB neurons. Green, anti-GFP; magenta, anti-nc82 (neuropile marker).

D) Representative confocal stack of a female *VGlut-AD (82986); 23E10-DBD>UAS-mCD8GFP* brain. Yellow and red arrows show non-dFB neurons. Green, anti-GFP; magenta, anti-nc82 (neuropile marker).

S19 Fig. Additional data for optogenetic activation of dFB$^{VGlut\cap 84C10}$ and dFB$^{ChAT\cap 84C10}$ neurons.

A) Box plots of total sleep change in % for female control (Empty-Split), VGlut-AD; 84C10-DBD, and 84C10-AD; ChAT-DBD flies expressing CsChrimson under standard optogenetic activation (5ms LED ON, 95ms LED OFF, with a 4 second delay between pulses). Two-way ANOVA followed by Sidak's multiple comparisons found no difference. n.s.= not significant. n=12-36 flies per genotype and condition.

B) Box plots of total sleep change in % for female control (Empty-Split), VGlut-AD; 84C10-DBD, and 84C10-AD; ChAT-DBD flies expressing CsChrimson under 20Hz activation. Two-way ANOVA followed by Sidak's multiple comparisons found that total sleep is increased in *84C10-AD; ChAT-DBD>CsChrimson*. n.s.= not significant, ****P<0.0001. n=19-26 flies per genotype and condition.

C) Box plots of nighttime sleep change in % ((nighttime sleep on activation day-nighttime sleep on baseline day/nighttime sleep on baseline day) X 100) for control (*Empty-Split>CsChrimson*), *VGlut-AD; 84C10-DBD>CsChrimson* and *84C10-AD; ChAT-DBD>CsChrimson* female flies presented in Fig 5H-5K. Two-way ANOVA followed by Sidak's multiple comparisons revealed that activating 84C10-AD; ChAT-DBD neurons significantly increases nighttime sleep. n.s.= not significant, ****P<0.0001. n=32-47 flies per genotype and condition.

D) Box plots of daytime sleep bout numbers for retinal-fed flies presented in Fig 5K. Two-way repeated measures ANOVA followed by Sidak's multiple comparisons test found that daytime sleep bout numbers are significantly increased in *VGlut-AD; 84C10-DBD>CsChrimson* and significantly decreased in *84C10-AD; ChAT-DBD>CsChrimson* female flies that are stimulated with 627nm LEDs. n.s.= not significant, **P<0.01, ****P<0.0001. n=33-47 flies per genotype.

E) Box plots of daytime sleep bout duration for retinal-fed flies presented in Fig 5K. Two-way repeated measures ANOVA followed by Sidak's multiple comparisons test found that daytime sleep bout duration is significantly increased in *84C10-AD; ChAT-DBD>CsChrimson* female flies. n.s.= not significant, ****P<0.0001. n=33-47 flies per genotype.

F) Box plots of locomotor activity counts per minute awake for retinal-fed flies presented in Fig 5K. Two-way repeated measures ANOVA followed by Sidak's multiple comparisons revealed that activating 84C10-AD; ChAT-DBD neurons significantly increases locomotion when the flies are awake. n.s.= not significant, **P<0.01, ****P<0.0001. n=33-47 flies per genotype.

G) Box plots of nighttime sleep bout numbers for retinal-fed flies presented in Fig 5K. Two-way repeated measures ANOVA followed by Sidak's multiple comparisons test found that nighttime sleep bout numbers are significantly increased in *VGlut-AD; 84C10-DBD>CsChrimson* and significantly decreased in *84C10-AD; ChAT-DBD>CsChrimson* female flies that are stimulated with 627nm LEDs. n.s.= not significant, **P<0.01, ****P<0.0001. n=33-47 flies per genotype.

H) Box plots of nighttime sleep bout duration for retinal-fed flies presented in Fig 5K. Two-way repeated measures ANOVA followed by Sidak's multiple comparisons test found that nighttime sleep bout duration is significantly increased in *84C10-AD; ChAT-DBD>CsChrimson* female flies. n.s.= not significant, *P<0.05, ****P<0.0001. n=33-47 flies per genotype.

I) Box plots of daytime sleep bout numbers for vehicle-fed flies presented in Fig 5K. Two-way repeated measures ANOVA followed by Sidak's multiple comparisons test. n.s.= not significant, *P<0.05. n=32-45 flies per genotype.

J) Box plots of daytime sleep bout duration for vehicle-fed flies presented in Fig 5K. Two-way repeated measures ANOVA followed by Sidak's multiple comparisons test. n.s.= not significant. n=32-45 flies per genotype.

K) Box plots of locomotor activity counts per minute awake for vehicle-fed flies presented in Fig 5K. Two-way repeated measures ANOVA followed by Sidak's multiple comparisons test. n.s.= not significant, *P<0.05. n=32-45 flies per genotype.

L) Box plots of nighttime sleep bout numbers for vehicle-fed flies presented in Fig 5K. Two-way repeated measures ANOVA followed by Sidak's multiple comparisons test. n.s.= not significant, ****P<0.0001. n=32-45 flies per genotype.

M) Box plots of nighttime sleep bout duration for vehicle-fed flies presented in Fig 5K. Two-way repeated measures ANOVA followed by Sidak's multiple comparisons test. n.s.= not significant, ****P<0.0001. n=32-45 flies per genotype.

The raw data underlying parts A, B, C, D, E, F, G, H, I, J, K, L, and M can be found in S1 Data.

S20 Fig. Multibeam data for optogenetic activation of dFB$^{VGlut\cap 84C10}$ and dFB$^{ChAT\cap 84C10}$ neurons at 50Hz.

A) Sleep profile in minutes of sleep per hour for day 2 (LED OFF, blue line) and day 3 (LED ON, red line) for retinal-fed Empty-Split control females expressing CsChrimson subjected to a 50Hz optogenetic activation protocol (cycles of 5ms LED ON, 15ms LED OFF) obtained with the DAM5H multibeam system.

B) Sleep profile in minutes of sleep per hour for day 2 (LED OFF, blue line) and day 3 (LED ON, red line) for retinal-fed *VGlut-AD; 84C10-DBD>CsChrimson* female flies subjected to a 50Hz optogenetic activation protocol (cycles of 5ms LED ON, 15ms LED OFF) obtained with the DAM5H multibeam system.

C) Sleep profile in minutes of sleep per hour for day 2 (LED OFF, blue line) and day 3 (LED ON, red line) for retinal-fed *84C10-AD; ChAT-DBD>CsChrimson* female flies subjected to a 50Hz optogenetic activation protocol (cycles of 5ms LED ON, 15ms LED OFF) obtained with the DAM5H multibeam system.

D) Box plots of total sleep change in % ((total sleep on activation day-total sleep on baseline day/total sleep on baseline day) X 100) obtained with the DAM5H system for control (*Empty-Split>CsChrimson*), *VGlut-AD; 84C10-DBD>CsChrimson* and *84C10-AD; ChAT-DBD>CsChrimson* female flies under a 50Hz optogenetic activation protocol. Two-way ANOVA followed by Sidak's multiple comparisons revealed that activating 84C10-AD; ChAT-DBD neurons significantly increases total sleep. n.s.= not significant, ****P<0.0001. n=19-29 flies per genotype and condition.

The raw data underlying part D can be found in S1 Data.

S21 Fig. Cholinergic and glutamatergic transmission in dFB neurons.

A) Sleep profile in minutes of sleep per hour for Empty-Split control, VGlut-AD; 84C10-DBD and 84C10-AD; ChAT-DBD females expressing RNAi against VAChT (80435 and 27684) and VGlut (40927 and 40845).

B) Box plots of total sleep (in minutes) for flies presented in A. One-way ANOVA followed by Tukey's multiple comparisons for each individual RNAi line. n.s.= not significant, **P<0.01, ****P<0.0001. n=20-68 flies per genotype.

C) Box plots of locomotor activity counts per minute awake for flies presented in A. Kruskal-Wallis ANOVA followed by Dunn's multiple comparisons for each individual RNAi line. n.s.= not significant, *P<0.05, **P<0.01. n=20-68 flies per genotype.

D) Box plots of total sleep change in % for female control (Empty-Split), VGlut-AD; 84C10-DBD, and 84C10-AD; ChAT-DBD flies expressing CsChrimson and RNAi against GFP (control), VAChT (line 27684) or VGlut (line 40845) under 50Hz activation. Two-way ANOVA followed by Sidak's multiple comparisons for each individual RNAi line. n.s.= not significant, *P<0.05, ***P<0.001, ****P<0.0001. n=15-43 flies per genotype and condition.

The raw data underlying parts B, C, and D can be found in S1 Data.

S1 Table: Description of FBS lines.

Identification of the AD construct combined with 23E10-DBD in each FBS line. Average number ± SEM and range of dFB neurons labeled by each line. Bowtie-VNC-SP (Y/N) indicates whether "bowtie" processes are seen in the brain and VNC-SP cell bodies are present in the VNC, Y= yes, N= no. Range of additional (non-dFB) neurons labeled in the brain of each line. Average number ± SEM of VNC metathoracic cells labeled by each FBS line. TPN1 (Y/N) indicates whether TPN1 neurons are present in the expression pattern, Y= yes, N= no. Range of additional cells in the VNC include any VNC neurons that is not TPN1 or VNC-SP.

The raw data underlying S1 Table can be found in S1 Data.

S2 Table: Summary of sleep phenotypes obtained for thermogenetic and optogenetic activation of FBS lines.
X indicates a significant increase between baseline and activation days, (+) indicates a significant increase compared with controls during thermogenetic activation, and (-) indicates a significant decrease.

S3 Table: List of fly stocks used in this study.

S1 Movie. Brain of a dFB-Split>UAS-GFP female.

S2 Movie. VNC of a dFB-Split>UAS-GFP female.

S3 Movie. Video of Cs flies showing different behaviors. Related to S15E Fig.
Example 10 minute video used to manually score fly behavior and correlate that with the behavior detected by the Trikinetics DAM5H multibeam system. Four Cs flies are shown with colored boxes to mark fly behavior. Feeding (black box) and grooming (yellow box) were detected by the multibeam as counts (movement within a single beam). Walking behavior (not marked) was detected by the multibeam as moves (movement from one beam to another). Resting (white box) is detected by the multibeam as an absence of counts or moves. Two behaviors, proboscis extension and single leg movement (both red boxes) were not detected as movement by the multibeam instead being recorded as rest.

S4 Movie. Video of a Cs fly performing a posture change. Related to S15 Fig.
Four Cs flies are shown with colored boxes to mark different fly behaviors. Feeding (black box), grooming (yellow box) were detected by the multibeam as counts (movement within a single beam). Walking behavior (not marked) was detected by the multibeam as moves (movement from one beam to another). Resting (white box) is detected by the multibeam as an absence of counts or moves. Posture change (blue box) was detected by the multibeam as counts (movement within a single beam).

S5 Movie. Video of Empty-AD; 23E10-DBD>CsChrimson fly behavior under baseline conditions. Video #1, control flies #1-4

S6 Movie. Video of Empty-AD; 23E10-DBD>CsChrimson fly behavior under LEDs ON activation conditions. Video #1, control flies #1-4

S7 Movie. Video of Empty-AD; 23E10-DBD>CsChrimson fly behavior under baseline conditions. Video #2, control fly #5

S8 Movie. Video of Empty-AD; 23E10-DBD>CsChrimson fly behavior under LEDs ON activation conditions. Video #2, control fly #5

S9 Movie. Video of Empty-AD; 23E10-DBD>CsChrimson fly behavior under baseline conditions. Video #3, control flies #6-9

S10 Movie. Video of Empty-AD; 23E10-DBD>CsChrimson fly behavior under LEDs ON activation conditions. Video #3, control flies #6-9

S11 Movie. Video of Empty-AD; 23E10-DBD>CsChrimson fly behavior under baseline conditions. Video #4, control flies #10-11

S12 Movie. Video of Empty-AD; 23E10-DBD>CsChrimson fly behavior under LEDs ON activation conditions. Video #4, control flies #10-11

S13 Movie. Video of flies expressing CsChrimson in dFB-Split neurons under baseline conditions. Video #1, dFB-Split flies #1-3

S14 Movie. Video of flies expressing CsChrimson in dFB-Split neurons under LEDs ON activation conditions. Video #1, dFB-Split flies #1-3

S15 Movie. Video of flies expressing CsChrimson in dFB-Split neurons under baseline conditions. Video #2, dFB-Split flies #4-5

S16 Movie. Video of flies expressing CsChrimson in dFB-Split neurons under LEDs ON activation conditions. Video #2, dFB-Split flies #4-5

S17 Movie. Video of flies expressing CsChrimson in dFB-Split neurons under baseline conditions. Video #3, dFB-Split flies #6-9

S18 Movie. Video of flies expressing CsChrimson in dFB-Split neurons under LEDs ON activation conditions. Video #3, dFB-Split flies #6-9

S19 Movie. Brain of a 84C10AD; ChAT-DBD>UAS-GFP female.

S20 Movie. VNC of a 84C10AD; ChAT-DBD>UAS-GFP female.

S21 Movie. Brain of a VGlut-AD; 84C10-DBD>UAS-GFP female.

S22 Movie. VNC of a VGlut-AD; 84C10-DBD>UAS-GFP female.

S23 Movie. Brain of a VGlut-AD (84713); 23E10-DBD>UAS-GFP female.

S24 Movie. Brain of a VGlut-AD (82986); 23E10-DBD>UAS-GFP female.

S1 Data: Raw data underlying all Figs.

A

Diagram of Thermogenetic and Optogenetic screens

For Optogenetic
Vehicle-Fed>Control
Retinal-Fed>Activation

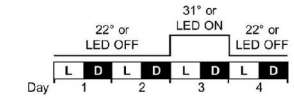

$$\text{Total Sleep Change (\%)} = \frac{\text{Total Sleep on Day3- Day2}}{\text{Total Sleep on Day2}} \times 100$$

B

Thermogenetic screen

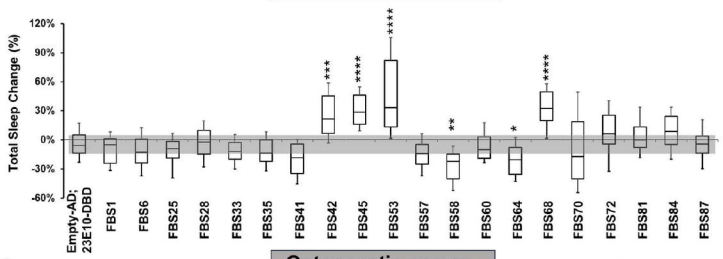

C

Optogenetic screen-Standard protocol

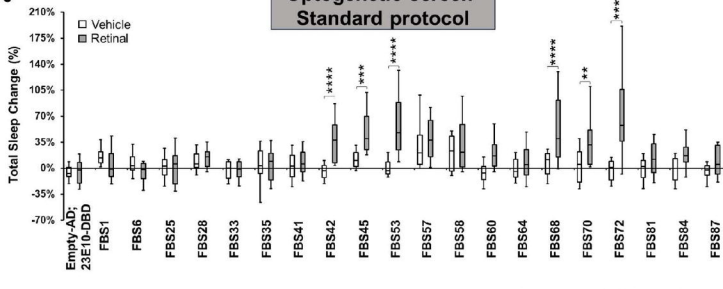

D

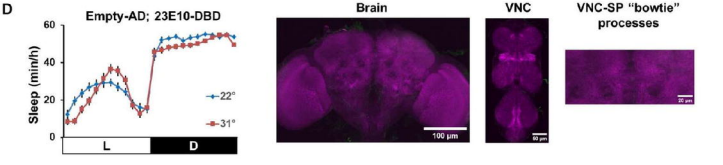

E

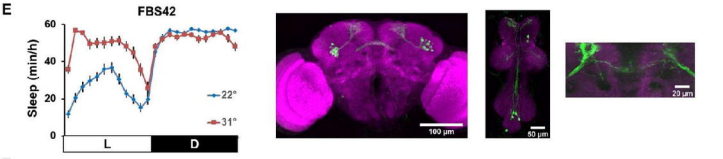

F

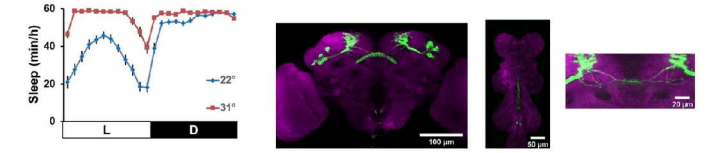

G

H

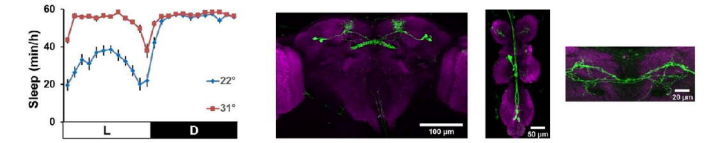

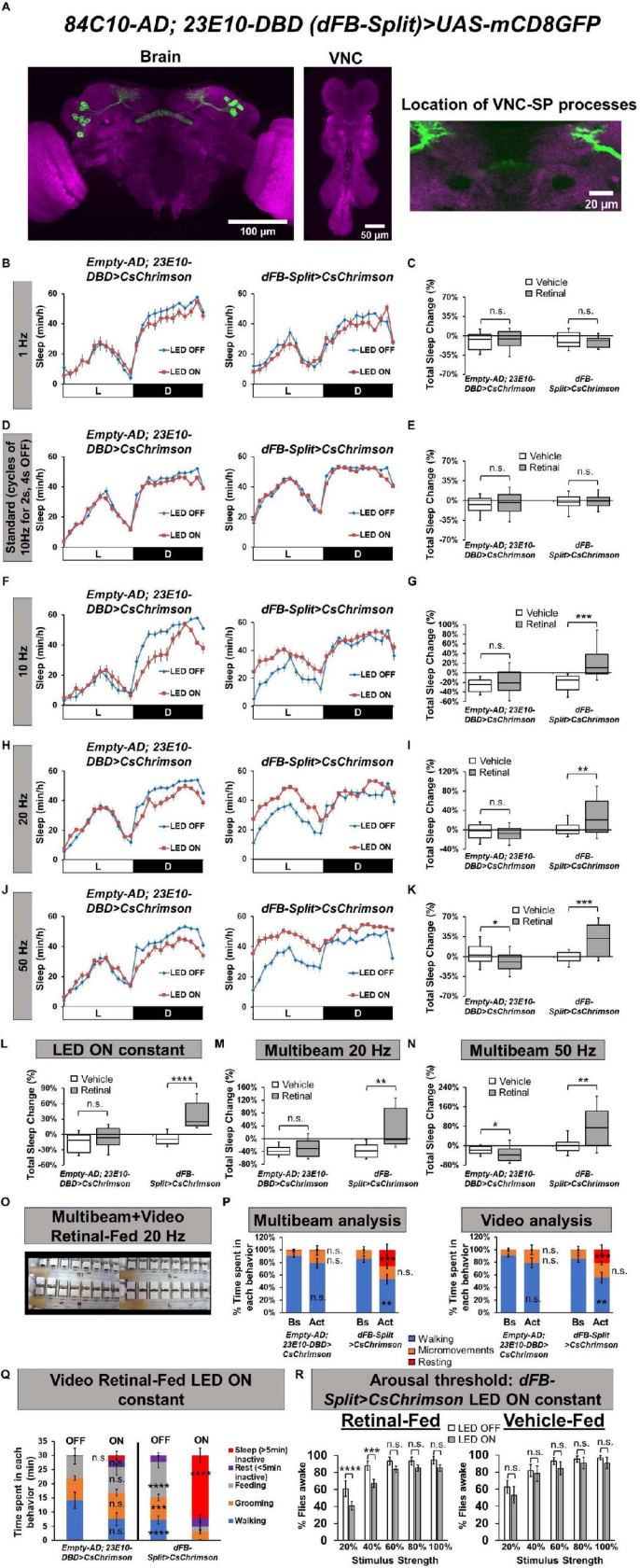
A
84C10-AD; 23E10-DBD (dFB-Split)>UAS-mCD8GFP
Brain
VNC
100 µm
50 µm
Location of VNC-SP processes
20 µm
B
Empty-AD; 23E10-DBD>CsChrimson
dFB-Split>CsChrimson
1 Hz
Sleep (min/h)
LED OFF
LED ON
L
D
C
Vehicle
Retinal
Total Sleep Change (%)
n.s.
Empty-AD; 23E10-DBD>CsChrimson
dFB-Split>CsChrimson
D
Standard (cycles of 10Hz for 2s, 4s OFF)
E
F
10 Hz
G
***
H
20 Hz
I
**
J
50 Hz
K
*
L
LED ON constant
****
M
Multibeam 20 Hz
N
Multibeam 50 Hz
O
Multibeam+Video Retinal-Fed 20 Hz
P
Multibeam analysis
Video analysis
% Time spent in each behavior
Bs
Act
Walking
Micromovements
Resting
Q
Video Retinal-Fed LED ON constant
Time spent in each behavior (min)
OFF
ON
Sleep (>5min inactive
Rest (<5min inactive)
Feeding
Grooming
Walking
R
Arousal threshold: dFB-Split>CsChrimson LED ON constant
Retinal-Fed
Vehicle-Fed
LED OFF
LED ON
% Flies awake
20%
40%
60%
80%
100%
Stimulus Strength

A

Courtship LTM Consolidation Protocol

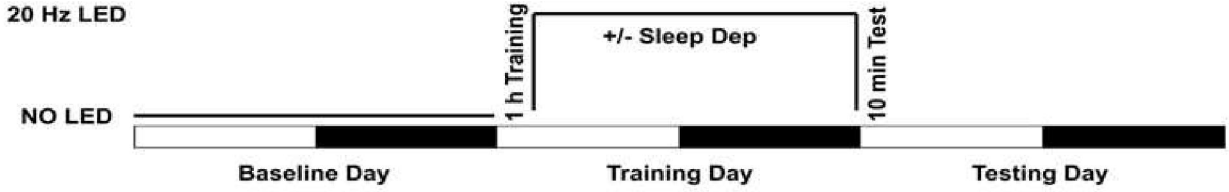

B

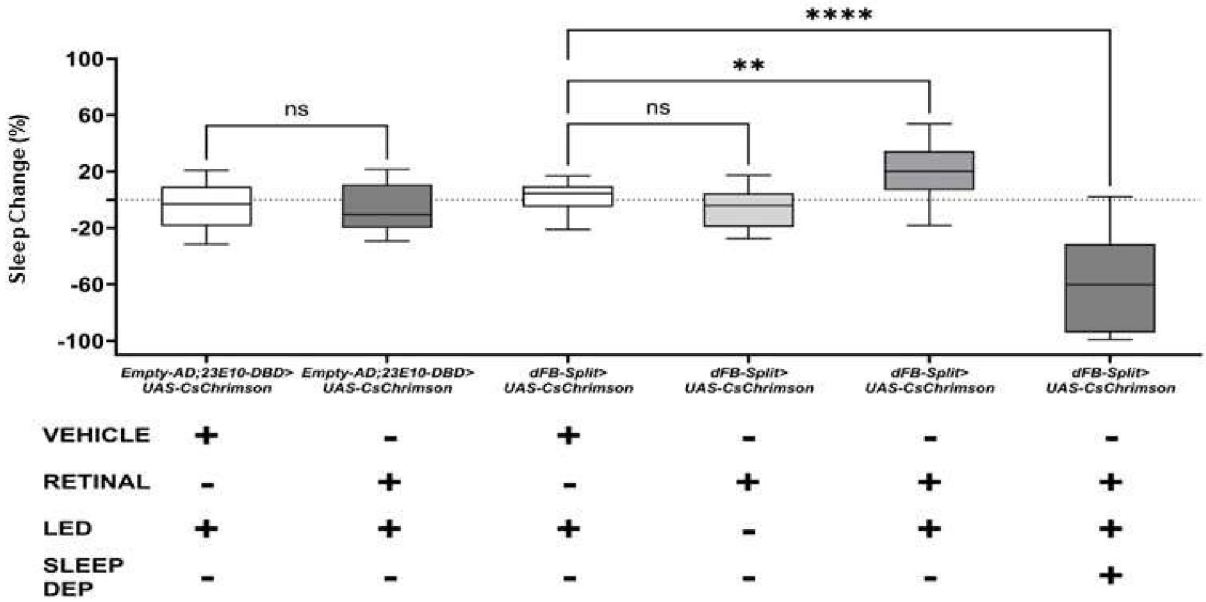

C

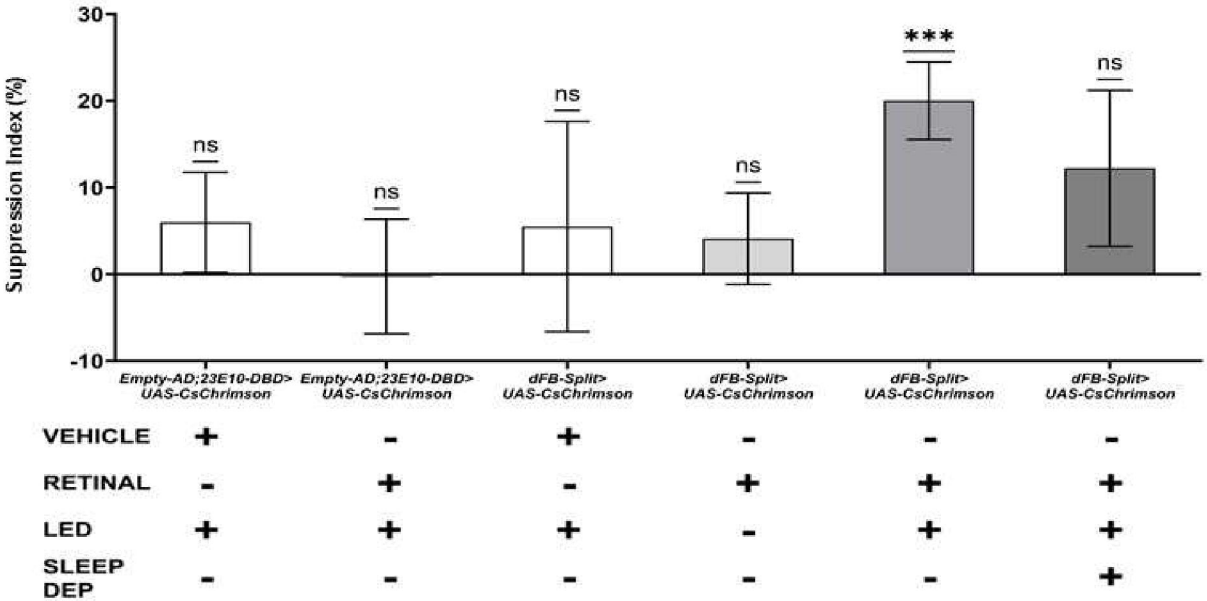

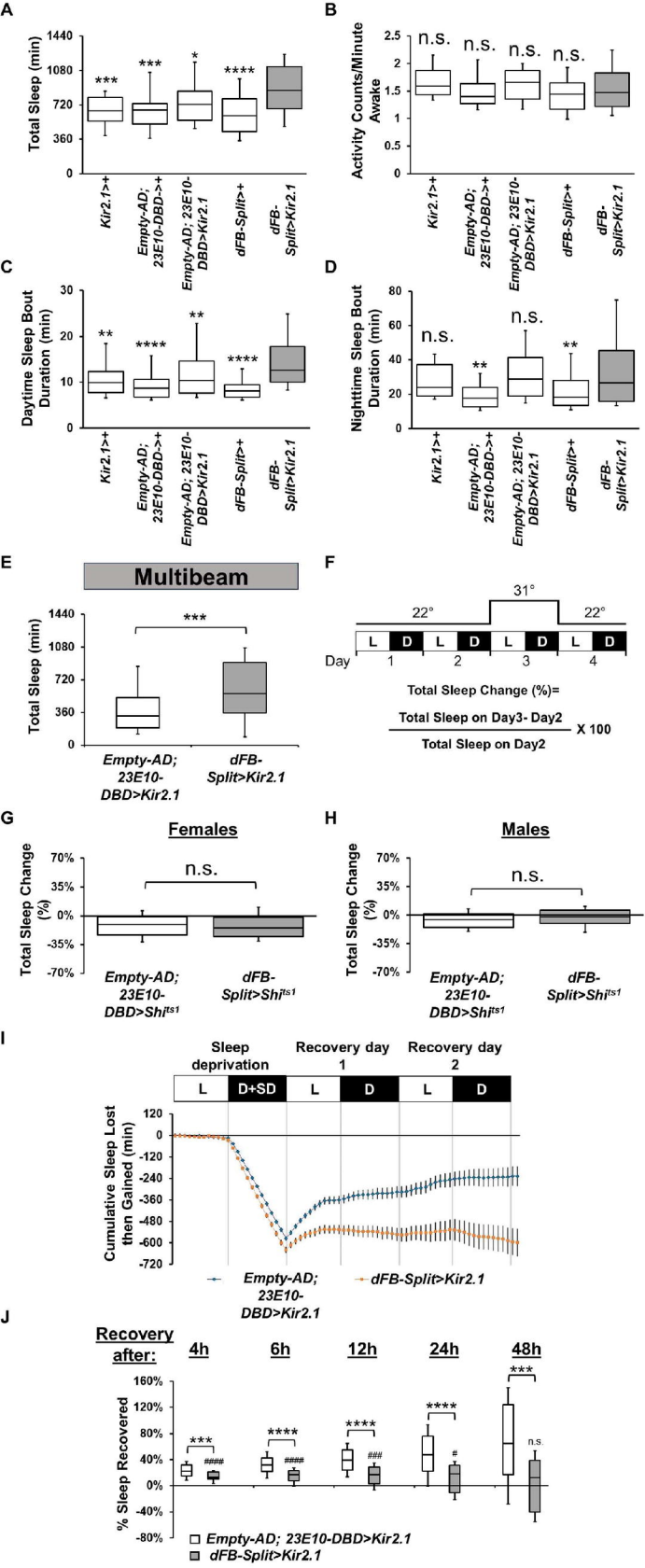
A
Total Sleep (min)
1440
1080
720
360
0
***
***
*
****
Kir2.1>+
Empty-AD; 23E10-DBD->+
Empty-AD; 23E10-DBD>Kir2.1
dFB-Split>+
dFB-Split>Kir2.1
B
Activity Counts/Minute Awake
2.5
2
1.5
1
0.5
0
n.s.
n.s.
n.s.
n.s.
Kir2.1>+
Empty-AD; 23E10-DBD->+
Empty-AD; 23E10-DBD>Kir2.1
dFB-Split>+
dFB-Split>Kir2.1
C
Daytime Sleep Bout Duration (min)
30
20
10
0
**
****
**
****
Kir2.1>+
Empty-AD; 23E10-DBD->+
Empty-AD; 23E10-DBD>Kir2.1
dFB-Split>+
dFB-Split>Kir2.1
D
Nighttime Sleep Bout Duration (min)
80
60
40
20
0
n.s.
**
n.s.
**
Kir2.1>+
Empty-AD; 23E10-DBD->+
Empty-AD; 23E10-DBD>Kir2.1
dFB-Split>+
dFB-Split>Kir2.1
E
Multibeam
Total Sleep (min)
1440
1080
720
360
0
***
Empty-AD; 23E10-DBD>Kir2.1
dFB-Split>Kir2.1
F
31°
22°
22°
L
D
L
D
L
D
L
D
Day
1
2
3
4
Total Sleep Change (%)=
Total Sleep on Day3- Day2
Total Sleep on Day2
X 100
G
Females
Total Sleep Change (%)
70%
35%
0%
-35%
-70%
n.s.
Empty-AD; 23E10-DBD>Shi^ts1
dFB-Split>Shi^ts1
H
Males
Total Sleep Change (%)
70%
35%
0%
-35%
-70%
n.s.
Empty-AD; 23E10-DBD>Shi^ts1
dFB-Split>Shi^ts1
I
Sleep deprivation
Recovery day 1
Recovery day 2
L
D+SD
L
D
L
D
Cumulative Sleep Lost then Gained (min)
120
0
-120
-240
-360
-480
-600
-720
Empty-AD; 23E10-DBD>Kir2.1
dFB-Split>Kir2.1
J
Recovery after:
4h
6h
12h
24h
48h
% Sleep Recovered
160%
120%
80%
40%
0%
-40%
-80%
***
####
****
####
****
###
****
#
***
n.s.
Empty-AD; 23E10-DBD>Kir2.1
dFB-Split>Kir2.1

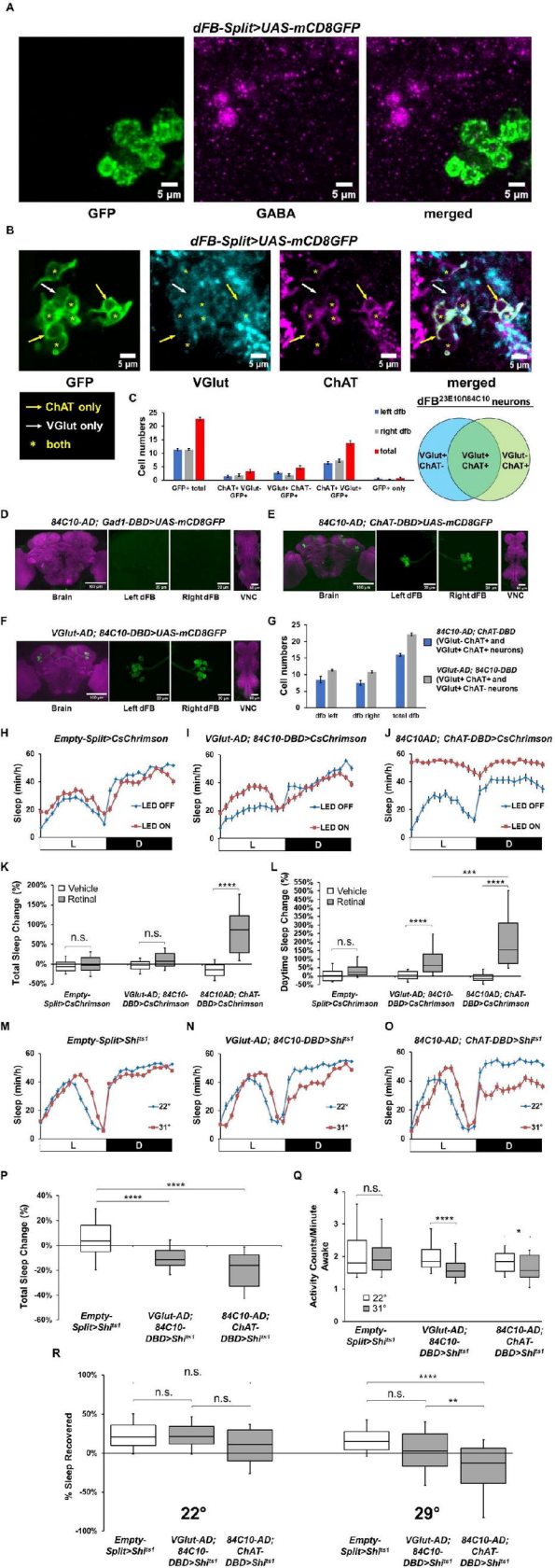
A
dFB-Split>UAS-mCD8GFP
5 µm
GFP
GABA
merged
B
dFB-Split>UAS-mCD8GFP
GFP
VGlut
ChAT
merged
ChAT only
VGlut only
both
C
Cell numbers
left dfb
right dfb
total
GFP+ total
ChAT+ VGlut- GFP+
VGlut+ ChAT- GFP+
ChAT+ VGlut+ GFP+
GFP+ only
dFB23E10∩84C10 neurons
VGlut+ ChAT-
VGlut+ ChAT+
VGlut- ChAT+
D
84C10-AD; Gad1-DBD>UAS-mCD8GFP
Brain
Left dFB
Right dFB
VNC
E
84C10-AD; ChAT-DBD>UAS-mCD8GFP
Brain
Left dFB
Right dFB
VNC
F
VGlut-AD; 84C10-DBD>UAS-mCD8GFP
Brain
Left dFB
Right dFB
VNC
G
Cell numbers
dfb left
dfb right
total dfb
84C10-AD; ChAT-DBD (VGlut- ChAT+ and VGlut+ ChAT+ neurons)
VGlut-AD; 84C10-DBD (VGlut+ ChAT+ and VGlut+ ChAT- neurons
H
Empty-Split>CsChrimson
Sleep (min/h)
LED OFF
LED ON
L
D
I
VGlut-AD; 84C10-DBD>CsChrimson
J
84C10AD; ChAT-DBD>CsChrimson
K
Total Sleep Change (%)
Vehicle
Retinal
n.s.
n.s.
****
Empty-Split>CsChrimson
VGlut-AD; 84C10-DBD>CsChrimson
84C10AD; ChAT-DBD>CsChrimson
L
Daytime Sleep Change (%)
n.s.
****
***
****
M
Empty-Split>Shits1
22°
31°
N
VGlut-AD; 84C10-DBD>Shits1
O
84C10-AD; ChAT-DBD>Shits1
P
Total Sleep Change (%)
****
****
Empty-Split>Shits1
VGlut-AD; 84C10-DBD>Shits1
84C10-AD; ChAT-DBD>Shits1
Q
Activity Counts/Minute Awake
n.s.
****
*
22°
31°
R
% Sleep Recovered
n.s.
n.s.
n.s.
****
n.s.
**
22°
29°